Acta Cryst. (1990). A46, 321-343

Modern Equations of Diffractometry. Goniometry*

BY D.J. THOMAS †

Medical Research Council Laboratory of Molecular Biology, Hills Road, Cambridge CB2 2QH, England

(*Received* 15 *June* 1989; *accepted* 10 *September* 1989)

Abstract

The various settings of a goniostat can best be calculated using a coordinate-free abstract operator notation. Concepts such as free axes, signed axes, angles and finite rotations are defined here using modern geometrical methods, and virtualized methods of describing combinations of rotations and of solving goniometric equations are given. These have the advantages of simplifying analysis and of being applicable to all types of machine. Three practical examples appropriate to the use of an area-detector diffractometer are presented: the synthesis of true precession motions using the concept of a 'virtual goniostat'; the generation of convenient crystal-viewing positions; and the solution of the equation of diffraction for the generalized, non-normal beam, rotation method. Algorithmic solutions are quoted in all three cases, corresponding to the code used on the FAST system at Cambridge and to that released to the EEC Cooperative Workshop on Position-Sensitive Detector Software in Paris in 1986. The emphasis has been placed on simple and reliable methods of computation. In each case, the equations reduce to the same, fundamental, form, containing four behaviourally distinct terms: one variable, one invariant, one odd and one even. The classical quaternion notation of theoretical physics, motor algebra and applications of dual numbers are also discussed.

1. Introduction

Rotations are conceptually very simple, and yet it is a common experience that rotational computations are tedious, difficult and prone to error. In this paper I propose a coordinate-free geometrical interpretation, annotated and analysed using a set of abstract operators. In this way the structure of the equations can be seen very clearly, without being obscured by the minutiae of a component notation. The emphasis is placed on general, reliable and quick methods of computation, not for abstruse questions and artificial problems, but for calculations that must be performed routinely in the field of diffractometry. The equations presented here are simultaneously the most general expounded so far in this field, being applicable to every kind of diffractometer, and yet are also uniquely simple in form. It has been necessary to develop a new notation to achieve this, but the attendant unfamiliarity is soon overcome by a few practical calculations using it.

To a large extent the present paper breaks with tradition, and although we must discuss conventional methods to place it in context, it is not necessary to be familiar with the more advanced topics in the literature in order to understand the new methods presented here. In fact, a major part of the considerable body of literature on the analysis of rotations continues a futile debate on whether or not the rather unapproachable quaternion notation is the best way to describe rotations in three-dimensional space. This has to be addressed in order to see how to continue. There are two distinct aspects to be considered: analysis and computation.

Historically, our modern analytic understanding of rotations arose from a desire to achieve a simple mathematical description of orientation and an interpretation, in particular, of the way in which rotations combine. Euler (1775*a*) is credited with a method of describing orientation, in terms of three angles, that survives to this day, particularly in engineering applications (often as Tait–Bryan angles), though there remains no consensus on their precise definition (Goldstein, 1950 or 1980, §4–4). Hamilton (1843*a*, *b*; 1844) is said to have solved the problem of combining rotations by observing that he needed three independent quantities, $\mathbf{i}$, $\mathbf{j}$ and $\mathbf{k}$ (see Table 1 for symbols used in this section), which satisfy $\mathbf{i}^2 = \mathbf{j}^2 = \mathbf{k}^2 = \mathbf{ijk} = -1$, though his equation for the combination of sequentially applied rotations had already been obtained by Gauss in 1819 (published posthumously in 1900). Indeed, Rodrigues published a correct tetravariate form earlier, in 1840. A precise modern definition of Hamilton's quaternion algebra is given by Dimitrić & Goldsmith (1989). Although Goldstein (1980, footnote at bottom of p. 156) describes quaternions as 'somewhat musty mathematics', they are still widely used in the form of Pauli spin matrices to execute transformations in the spinor calculus essential to modern physics. The related Cayley–Klein parameters are, indeed, still sometimes used (Goldstein, 1950 or 1980, §4-5). The extra variable is used to achieve a homogeneous structure (Diamond, 1988), which can be very convenient analytically (Klein, 1884*b*). Although complex numbers dominate modern analysis, engineers have

* *Editorial note*: This paper was typeset from electronic input supplied by the author using the widely available text formatting program TEX developed by D.E. Knuth, Stanford University, USA. Authors wishing to assist the Technical Editor with experimental use of TEX should contact the Technical Editor's office before submitting a manuscript.

† Present address: European Molecular Biology Laboratory, Meyerhofstrasse 1, Postfach 10.2209, D-6900 Heidelberg, Federal Republic of Germany.

0108-7673/90/050321-23$03.00

Table 1. *Symbol table for* §1

$\mathcal{E}$	even function in principal equation of goniometry
$\mathcal{I}$	invariant term in principal equation of goniometry
i, j, k	the generators of Hamilton's quaternion algebra.
l, m, n	direction cosines
λ, μ, ν	Diamond's notation for the quaternion vector (Goldstein uses e_1, e_2, e_3)
$\mathcal{O}$	odd function in principal equation of goniometry
$\mathcal{V}$	variable in principal equation of goniometry
$\mathcal{W}$	a double-valued asymmetric radical form in the reduced form of the general solution
π	the irrational number 3·14159265···
σ	Diamond's notation for the quaternion scalar (Goldstein uses e_0)
ϖ	(curly pi) the non-trivial square-root of zero: $\varpi^2 = 0, \varpi \neq 0$ (more usually ϵ or ω)

resurrected the dual numbers ($a + \varpi b; \varpi^2 = 0, \varpi \neq 0$)* of Clifford (1873) as an aid to the practical analysis of complex mechanical linkages (Дименттберг, 1948; Denavit, 1958; Yang & Freudenstein, 1964; Yang, 1969), exploiting the commutative properties of numbers and quaternions (*e.g.* Hamilton, 1853) and the immediate termination of Maclaurin expansions containing ϖ to enable simultaneous analysis of rotation and translation. Indeed, the axes of a goniostat are properly represented by *motors* (Brand, 1947, Chapter II) but if all axes intersect the origin, we do not need this formalism. The modern interest in Clifford algebras and directed-number schemes has exposed a restrictive ambiguity in the use of complex numbers, so often used to contract rotational calculations, which is that they represent simultaneously a point in space and a rotation–dilatation operation (Hestenes, 1986). When the two functions are separated clearly, complex numbers are seen as a special (and rather degenerate) Clifford algebra. Real Clifford algebras in four dimensions can unify all of the tetravariate analyses of rotations in three dimensions, and are becoming important now because of their suitability to handle the rigours of various topics in theoretical physics.

In recent years, with the advent of digital computers, the emphasis has turned to the practical implementation of rotational calculations. In many cases, the most obvious representation, in terms of 3×3 positive orthogonal (*i.e.* real unitary) matrices is used, and justifiably so because fewer machine operations are needed than with most competing formulations. The analytical efficiency of the tetravariate half-angle (*i.e.* quaternion) formulations is not manifest when actually evaluating the effect of a rotation on an object, primarily not because multiplication by 2×2 complex matrices or 4×4 real matrices takes more operations than does multiplication by 3×3 matrices, but because all half-angle formulations necessarily mean that the primary rotation operator has to be applied not once, as is the case with 3×3 full-angle rotation matrices, but twice. Indeed, many texts simply state from the outset that rotations of vectors are expressed by an equation of the form $X' = RXR^*$ [see Misner, Thorne & Wheeler, 1973, equation (41.19), p. 1142] in which the vector, X, appears in the form of a 2×2 complex square matrix as if no other possibility existed; some do not explain even that much. The claims made in some texts for the quaternion formalism are therefore somewhat exaggerated;* this is particularly true when its extra analytic power is not needed, such as when the axes of the rotations are not variable quantities, as indeed is the case when using a diffractometer, when they are constants fixed at the time of manufacture.

Misner, Thorne & Wheeler (1973), probably following Klein, explain the occurrence of half-angles by mod-

* Clifford, Denavit and Дименттберг use $\omega^2 = 0$, whilst Brand, Yang and Freudenstein use $\epsilon^2 = 0$. The use of ϖ here is to avoid a conflict with other conventional meanings of ϵ and ω and does not reflect either common or recommended usage. Indeed, even the nowadays rare ϖ conflicts with Tait's (1890) widespread use of it in his standard work on quaternions as a general vector.

* See, for example, equation [24] in Blümlich & Spiess (1985), which requires 80 multiplications, 60 additions, 3 sines and 3 cosines to calculate the orientation resulting from rotations about principal axes of their representation. The authors ask us to note the simplicity of the calculation, whose result is left, inconveniently, in half-angle form, regardless of the fact that an equivalent general calculation using 3×3 matrices in full-angle notation would require only 54 multiplications, 36 additions and the same number of trigonometric calculations.

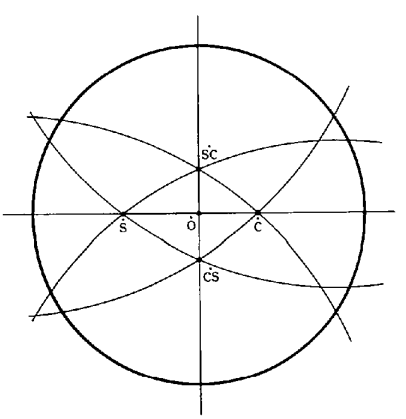

Fig. 1. A stereogram showing the occurrence of half-angles when determining axial orientations. It shows that the occurrence of halved angles is inevitable even without the contrived introduction of reflections. The author is grateful to Dr Robert Diamond for pointing out this construction. The annotation is chosen to match the discussion of the generation of precession motions in §9.

elling rotations by double reflections, and yet the idea that (*ex absurdo*!) an infinitesimally small rotation is best explained by two inversions of chirality is quite bizarre. Indeed, the set of reflections does not even form a group, whereas the set of rotations does, since the composition of two reflections is not another reflection, but a rotation (Klein, 1884*a*). A clearer demonstration of the inevitability of half-angles in the calculation of axial orientations is to be had by drawing the geometry out explicitly: here we use a stereogram (Fig. 1).

We start with two rotation axes, $\dot{s}$ and $\dot{c}$, and choose a certain angle of rotation, say $\angle s$ and $\angle c$, for each of them. We can operate these two rotations sequentially in either order, giving different results, shown by Rodrigues (1840) to have the same angle of rotation, but different axes, say $\dot{s}\dot{c}$ and $\dot{c}\dot{s}$. That these are, indeed, the axes of the resulting rotations can be established with certainty by noting that operation of the rotation ($\dot{\mathbf{s}}$) about $\dot{s}$ on $\dot{c}\dot{s}$ brings it into alignment with $\dot{s}\dot{c}$, and the subsequent operation of the rotation ($\dot{\mathbf{c}}$) about $\dot{c}$ brings it back to its original orientation, $\dot{c}\dot{s}$. Thus $\dot{c}\dot{s}$, being unaffected by the sequential operation of $\dot{\mathbf{s}}$ then $\dot{\mathbf{c}}$, must be the axis of the composite rotation. A similar construction applies for $\dot{s}\dot{c}$.

It is immediately clear that the great circle containing $\dot{s}$ and $\dot{c}$ bisects the angles $\angle\dot{c}\dot{s}\,\dot{s}\dot{c} = \angle s$ and $\angle\dot{s}\dot{c}\,\dot{c}\dot{s} = \angle c$ and that use must be made of these halved angles when determining the orientation of $\dot{s}\dot{c}$ or $\dot{c}\dot{s}$ by spherical trigonometry. Notwithstanding this, it turns out, as we shall see later, that if our primary concern is to calculate the effects of rotation, rather than merely to determine the orientation of a generated axis, we can only complicate our calculations by adopting a half-angle notation.

The intersection, $\dot{o}$, of the great circle containing $\dot{s}$ and $\dot{c}$ and the great circle containing $\dot{s}\dot{c}$ and $\dot{c}\dot{s}$ (placed for convenience at the zenith of the stereogram) is the axis of the rotation which would be produced if the two generating rotations were applied simultaneously. This is of relevance in the generation of precession motions discussed in §9.

2. A symmetry-based decomposition of the structure of rotation

To proceed further, we define two geometrical concepts: the line of stasis and the orbital plane. In any rigid-body motion, there is always a unique and well defined locus (set of points), not necessarily within the body, which has no velocity; points within the locus may translate along it, but the locus itself is (at least momentarily) stationary. This is a consequence of a proof credited to Chasles, who showed that the most general possible motion of a rigid body is a screw motion, itself a corollary of an earlier theorem of Euler (1758, 1765). I call this locus the line of stasis, and it corresponds with the instantaneous axis of rotation. In any normal representation of space, this line is locally straight. During purely rotational motions, points which are not in the line of stasis must execute an orbital motion around it, and I call the instantaneous plane of any such orbit the orbital plane. There are infinitely many such planes. Similarly, in any normal representation of space, these planes are locally flat and locally parallel. It is always possible to uncouple the translational part of a motion from the rotational, so our analysis has not been restricted by disregarding screw motions.

We describe the line of stasis and any ray intersecting it and contained within the orbital plane as mutually orthogonal. This must mean that in a Cartesian–Euclidean space they are normal to each other, and the angle between them is called a right angle. It is, however, a central theme of this paper that the behaviour of rotating objects can be made manifest without imposing a metric structure. This is quite unusual, and means that the approach here could be adopted into applied differential geometry, which has hitherto shunned rotations for want of a secure representation for them (Burke, 1985).

We also define three algebraic concepts. The first is a free axis, representable by $\overline{\mathrm{E}}$, which is identified with an unconstrained ability to rotate about a named axis or line of stasis. Closely related is the concept of a signed axis, representable by $\vec{\mathrm{E}}$, which differs only in having a specified sense of rotation which can be referred to as positive. These concepts are illustrated in Fig. 2. The term 'general axis', representable by $\dot{\mathrm{E}}$, can be used when the distinction need not be drawn. The signed axis is algebraically powerful, and indeed the solution of many real problems in goniometry depend upon its use. Additionally, it is the natural description of the properties of all commonly used numerical representations of the direction of axes of rotation.

The concepts of rotation, which we may represent by $\dot{\mathbf{E}}$, and angle, representable by $\angle e$, in this paper have their conventional meaning in Euclidean space. With these definitions, all of the principal equations of goniometry split into four behaviourally distinct components which we arrange as follows:

$$\mathcal{V} = \mathcal{I}(\dot{\mathrm{E}}) + \mathcal{O}(\vec{\mathrm{E}},\angle e) + \mathcal{E}(\dot{\mathrm{E}},\angle e). \qquad (2.1)$$

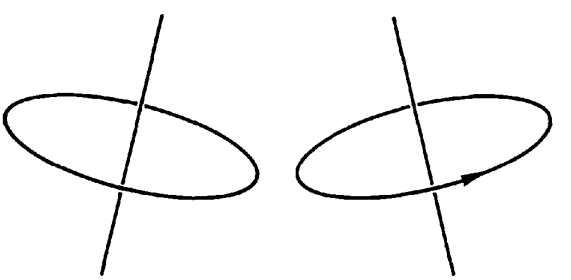

Fig. 2. A free axis and a signed axis. It is to be noted especially that a representation of the sense of rotation of an axis by means of a vector pointing along it is rigorously to be avoided. It is simpler, more reliable, and in no way less convenient to mark it by the direct means of an arrow wrapped around the line of stasis in one of the orbital planes. This technique draws heavily on the arguments to be found in Burke (1985) and ensures that the geometrical representation does not depend on an externally defined handedness of interpretation.

Table 2. *Symbol table for* §3

$\mathbf{I}$	the identity operator; also the identity matrix
$\dot{\mathrm{E}}$	a rotation axis
$\mathrm{E}\vert$	a rotation axis as a left-acting operator
$\vec{\mathrm{E}}$	a signed axis
$\overline{\mathrm{E}}$	a free or unsigned axis
$\vert\mathrm{E}$	a sixa, *i.e.* a rotation axis as a right-acting operator; geometrically dual to $\mathrm{E}\vert$
$\angle e$	an angle of rotation about $\vec{\mathrm{E}}$
$\nabla_{\angle e}$	an operator performing differentiation with respect to an angle of rotation
$\mathrm{E}\rfloor\overline{\mathrm{E}}$	the rotation symmetric operator
$\mathrm{E}\vert\overline{\mathrm{E}}$	the rotation antisymmetric operator
$\mathrm{E}\vert\mathrm{E}$	the rotation invariant operator
$\mathrm{E}\rfloor\mathrm{E}$	the rotation skew-symmetric operator
$\mathrm{E}\lfloor\mathrm{E}$	the inverse rotation skew-symmetric operator
$\acute{\mathrm{E}}$	a general or required rotation
$\mathbb{E}^3$	three-dimensional Euclidean space, also serving as a model for direct or reciprocal space
$\overline{\mathbb{E}}^3$	hand-inverted three-dimensional Euclidean space
exp	the exponential function, defined as a power series
$\circ$	composition (action of one operator after another)
$\blacksquare$	the correspondence or inner product
$\times$	used only to specify the size of matrices within the text
$\rightarrow$	a general mapping between sets

The function $\mathcal{E}$ is even with respect to both of its arguments, and the function $\mathcal{O}$ is odd with respect to both of its arguments. The function $\mathcal{I}$ is even with respect to its argument, but is called invariant because it does not depend on the angle of rotation, $\angle e$. The term $\mathcal{V}$ is variable and related to the particular application. The terms in (2.1) are general: for example, they match rotational operators in (3.6), but also match the scalar terms in (4.7) and (11.7). It is the matching of the behaviour (represented by the symmetries) of the right-hand side of (2.1) (representing the mechanics of our goniostat) to our specific experimental requirements represented on the left-hand side that forces our method to work. The simplifying power of this symmetry-based decomposition is the principal theme of this paper.

3. Algebraic representation by rotation operators

Algebraically, we can represent a rotation by an *operator* which has the form (see Table 2 for notation)

$$\acute{\mathbf{E}} = \acute{\mathbf{E}}(\vec{\mathrm{E}},\angle e)\colon \mathbb{E}^3 \rightarrow \mathbb{E}^3, \qquad (3.1)$$

in which the specification of the sense of rotation as the angle increases is encoded by the use of a signed axis, $\vec{\mathrm{E}}$. This equation reads: the operator $\acute{\mathbf{E}}$, which is a function of $\vec{\mathrm{E}}$ and of $\angle e$, maps Euclidean space autonomically (into itself). In general, the restriction to operation in Euclidean space is unnecessary, but it helps to focus the present discussion. In many circumstances, a matrix is a suitable representation of the action of an operator (*e.g.* Goldstein, 1980, p. 135). Some 3×3 matrix representations are discussed in §5, but the abstraction of operator notation allows a clearer view of the structure of the equations.

All of the properties of a system specific to a freedom of rotation about an axis must be representable as functions of that axis, representable by $\overline{\mathrm{E}}$, a free axis. When this axis is used as a passive algebraic entity (a right-multiplicand) which can be left-multiplied by an operator, or when it is used as an operator to right-multiply another form, it is properly a representation of an axis in the form of a left-acting operator, $\mathrm{E}\vert$, called just *axis* for short. It can equivalently be used actively as a left-multiplier or passively as a left-multiplicand, in which it is properly a representation of an axis in the form of a right-acting operator, $\vert\mathrm{E}$, which I choose to call *sixa* (*axis* backwards). The forms $\mathrm{E}\vert$ and $\vert\mathrm{E}$ are conjugate, and their notation, like the 'bra-ket' notation of Dirac (1958), is chosen deliberately to emphasize their equivalence and symmetry; every correct equation using them reads correctly in either direction. In some geometrical representations the two forms appear very different in function, but this is more a reflection of an inadequacy in the geometrical representation than of a true functional difference between $\mathrm{E}\vert$ and $\vert\mathrm{E}$ (see §13). With conventionally arranged notations, computational forms of $\mathrm{E}\vert$ and of $\vert\mathrm{E}$ are normally represented by column and row vectors respectively. However, one should not feel too strongly attached to these specific and restrictive computational representations.

All of the properties of a system specific to one particular angle of rotation can similarly be represented by a single algebraic symbol, which is skew-symmetric relative to that angle. The symmetry of 3.1 is such that we can start with one of two opposite forms, say $\mathrm{E}\rfloor\mathrm{E}$ and $\mathrm{E}\lfloor\mathrm{E}$. The double occurrence of the name of the rotation axis in the rotation operators is to assert that this notation comprehends the potential for half-angle factorization, even through a construction based on reflections.

Thus the existence of non-autonomic 'half-operators' like $\mathrm{E}\rfloor$ and $\lceil\mathrm{E}$ (so that, perhaps, $\mathrm{E}\rfloor\mathrm{E} = \mathrm{E}\rfloor \circ \lceil\mathrm{E}$; $\lceil\mathrm{E}: \mathbb{E}^3 \to \overline{\mathbb{E}}^3$, $\mathrm{E}\rfloor: \overline{\mathbb{E}}^3 \to \mathbb{E}^3$) is acknowledged and implied, though apart from $|\mathrm{E}$ and $\mathrm{E}|$ we shall neither use nor define them here. But the notation also declares that a metric-invariant differential structure exists for the operators (see §13); even if a metric-dependent representation is used for, say, $\mathrm{E}|$, one can think of one of the symbols as being in a multiplying position and the other in a dividing position, so that any potentially variable 'length' attaching to a representation of $\mathrm{E}|$ cancels completely and the operators remain strictly idempotent. In other words, the two occurrences are mutually contravariant. Indeed, geometrically, they are duals (see §13). This property is not always immediately obvious in computational representations of them. In fact, a little further thought will show that even the half-operators themselves must each contain the same double occurrence, so that in most computational representations of the full operators, a quadruple occurrence is seen.

I have chosen to call $\mathrm{E}\rfloor\mathrm{E}$ the rotation skew-symmetric operator and $\mathrm{E}\lfloor\mathrm{E}$ the inverse rotation skew-symmetric operator. Either can be used as generators of rotations, by making use of the power-series definition of the exponential function [*cf.* Goldstein (1980), equation (4–77), p. 157; or Misner, Thorne & Wheeler (1973), equation (41.17), p. 1141]

$$\dot{\mathbf{E}} = \exp(\angle e\, \mathrm{E}\rfloor\mathrm{E}), \tag{3.2}$$

in which $\angle e$, being just a real number, can commute with $\mathrm{E}\rfloor\mathrm{E}$. The skew-symmetric operator $\mathrm{E}\rfloor\mathrm{E}$ itself must necessarily behave in the manner of a classical imaginary (like $i = \sqrt{-1}$), in order to maintain the necessary unit normalization (*i.e.* non-scale-changing property) of the exponential. The skew operators $\mathrm{E}\rfloor\mathrm{E}$ and $\mathrm{E}\lfloor\mathrm{E}$ must therefore also repeat on every fourth power. It thus helps to expand our notation into a set of five operators in addition to the identity, whose compositional products satisfy the following system of equations:

$$\begin{pmatrix} \mathbf{I} \\ \mathrm{E}|\mathrm{E} \\ \mathrm{E}\rfloor\mathrm{E} \\ \mathrm{E}\lceil\mathrm{E} \\ \mathrm{E}\lfloor\mathrm{E} \end{pmatrix} \circ \begin{pmatrix} \mathbf{I} & \mathrm{E}|\mathrm{E} & \mathrm{E}\rfloor\mathrm{E} & \mathrm{E}\lceil\mathrm{E} & \mathrm{E}\lfloor\mathrm{E} & \mathrm{E}\lfloor\mathrm{E} \end{pmatrix}$$

$$= \begin{pmatrix} \mathbf{I} & \mathrm{E}|\mathrm{E} & \mathrm{E}\rfloor\mathrm{E} & \mathrm{E}\lceil\mathrm{E} & \mathrm{E}\lfloor\mathrm{E} & \mathrm{E}\lfloor\mathrm{E} \\ \mathrm{E}|\mathrm{E} & \mathrm{E}|\mathrm{E} & 0 & 0 & 0 & 0 \\ \mathrm{E}\rfloor\mathrm{E} & 0 & \mathrm{E}\rfloor\mathrm{E} & \mathrm{E}\lceil\mathrm{E} & \mathrm{E}\lfloor\mathrm{E} & \mathrm{E}\lfloor\mathrm{E} \\ \mathrm{E}\lceil\mathrm{E} & 0 & \mathrm{E}\lceil\mathrm{E} & \mathrm{E}\lceil\mathrm{E} & \mathrm{E}\lfloor\mathrm{E} & \mathrm{E}\lceil\mathrm{E} \\ \mathrm{E}\lfloor\mathrm{E} & 0 & \mathrm{E}\lfloor\mathrm{E} & \mathrm{E}\lfloor\mathrm{E} & \mathrm{E}\lceil\mathrm{E} & \mathrm{E}\lfloor\mathrm{E} \\ \mathrm{E}\lfloor\mathrm{E} & 0 & \mathrm{E}\lfloor\mathrm{E} & \mathrm{E}\lceil\mathrm{E} & \mathrm{E}\lfloor\mathrm{E} & \mathrm{E}\lfloor\mathrm{E} \end{pmatrix}. \tag{3.3}$$

Thus the operators $\mathbf{I}$, $\mathrm{E}|\mathrm{E}$ and $\mathrm{E}\lfloor\mathrm{E}$ are idempotent, whilst $\mathrm{E}\rfloor\mathrm{E}$ is equal to all of its odd powers, and all of its even powers are $\mathrm{E}\lfloor\mathrm{E}$. The invariant

$$\mathrm{E}|\mathrm{E} \equiv \mathrm{E}| \circ |\mathrm{E} \tag{3.4}$$

and the symmetric

$$\mathrm{E}\lfloor\mathrm{E} \equiv \mathbf{I} - \mathrm{E}|\mathrm{E} \tag{3.5}$$

are even with respect to $\dot{\mathrm{E}}$ (representable by either $\overline{\mathrm{E}}$ or $\vec{\mathrm{E}}$) but $\mathrm{E}\rfloor\mathrm{E}$, which depends on the sense of rotation, must be specifically related to $\vec{\mathrm{E}}$. Detailed computational representations of these operators as 3×3 matrices are given in §5 and a simple diagram giving an intuitive description of the action of the major operators on a general vector is displayed as Fig. 3.

Throughout this paper, we distinguish between skew-symmetry, which is used to describe terms having the same symmetry as does a rotation through a right angle in Cartesian–Euclidean space, and anti-symmetry, which is used to describe terms having the same symmetry as a rotation through half of a revolution in Cartesian–Euclidean space. The conventionally defined symmetries of matrices used to represent rotations are higher than those of the rotations they represent, and are not generally used here.

Formally, it is $\mathbf{I}$ and $\cdot\rfloor\cdot$ (which embodies the skew-symmetric properties) which are the most fundamental quantities from which all of the others (including axes and sixas) derive. However, the links between the various operators are so strong that for all practical purposes we can derive our computational forms from any defining subset.

From the relations above, which imply trivially that $(\mathrm{E}\rfloor\mathrm{E})^0 = \mathbf{I}$, that $(\mathrm{E}\rfloor\mathrm{E})^2 = \mathrm{E}\rfloor\mathrm{E} = -\mathrm{E}\lfloor\mathrm{E}$ and that $(\mathrm{E}\rfloor\mathrm{E})^{n+2} = -(\mathrm{E}\rfloor\mathrm{E})^n$ for all positive integers, n, (3.2) expands into

$$\begin{aligned} \dot{\mathbf{E}} &= (\mathbf{I} - \mathrm{E}|\mathrm{E}) + \mathrm{E}\rfloor\mathrm{E}\sin\angle e + \mathrm{E}\lfloor\mathrm{E}\cos\angle e \\ &= \mathrm{E}|\mathrm{E} + \mathrm{E}\rfloor\mathrm{E}\sin\angle e + \mathrm{E}\lfloor\mathrm{E}\cos\angle e, \end{aligned} \tag{3.6}$$

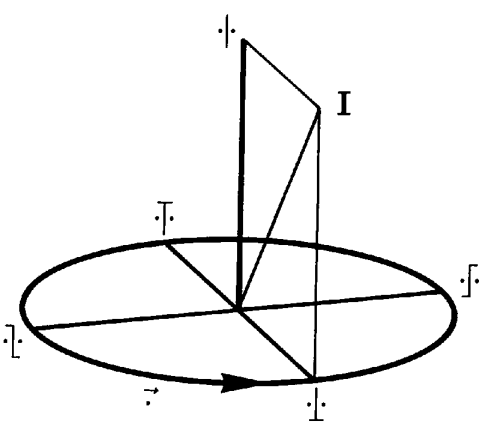

Fig. 3. An indicator diagram for the rotational operators. This shows how the invariant operator $\cdot|\cdot$ projects its vector argument onto the line of stasis, and that the skew operators $\cdot\rfloor\cdot$ and $\cdot\lfloor\cdot$ project their vector arguments onto the orbital plane with an attendant right rotation. The symmetric operator $\cdot\lfloor\cdot$ similarly projects onto the orbital plane, but with no attendant rotation, whilst the antisymmetric operator $\cdot\lceil\cdot$ projects with a rotation of half a turn. The identity operator, $\mathbf{I}$, marks the unaltered operand in its original position.

which has the same form as the behavioural decomposition of (2.1).

It is also useful to define a correspondence, or inner, product, ▪, whose action between rotational operators is specified completely by

$$\begin{pmatrix} \mathbf{I} \\ \mathrm{E}\rfloor\mathrm{E} \\ \mathrm{E}\lfloor\mathrm{E} \\ \mathrm{E}\rceil\mathrm{E} \\ \mathrm{E}\lceil\mathrm{E} \\ \mathrm{E}\rfloor\mathrm{E} \end{pmatrix} \blacksquare \begin{pmatrix} \mathbf{I} & \mathrm{E}\rfloor\mathrm{E} & \mathrm{E}\lfloor\mathrm{E} & \mathrm{E}\rceil\mathrm{E} & \mathrm{E}\lceil\mathrm{E} & \mathrm{E}\rfloor\mathrm{E} \end{pmatrix}$$

$$= \begin{pmatrix} +3 & +1 & 0 & -2 & 0 & +2 \\ +1 & +1 & 0 & 0 & 0 & 0 \\ 0 & 0 & +2 & 0 & -2 & 0 \\ -2 & 0 & 0 & +2 & 0 & -2 \\ 0 & 0 & -2 & 0 & +2 & 0 \\ +2 & 0 & 0 & -2 & 0 & +2 \end{pmatrix}, \quad (3.7)$$

which declares the ranks of the operators and the degree to which their actions correspond. It also exposes the two necessary antisymmetries: $\mathrm{E}\rfloor\mathrm{E} = -\mathrm{E}\lceil\mathrm{E}$ and $\mathrm{E}\lfloor\mathrm{E} = -\mathrm{E}\rceil\mathrm{E}$. If the result on the right-hand side is 0, the operators are regarded as independent or orthogonal; if it is 1, they correspond in a one-dimensional subspace corresponding to the line of stasis; if it is 2, they correspond in a two-dimensional subspace corresponding with the orbital plane; when it is 3, they correspond completely – a result which obtains only if both are the identity operator. The minus signs indicate the presence of a mutual antisymmetry in the sense defined above. One example of a computational representation of the correspondence product is given at the end of §5.

The correspondence product, ▪, can also be used between two axes or between two sixas, when it reduces to the ordinary scalar operation of sixa on axis:

$$1|\blacksquare 2| \equiv |2\blacksquare|1 \equiv |12| \equiv |21|, \quad (3.8)$$

which often allows it to be eliminated (or incorporated) by trivial rearrangement, as in, for example, (4.13).

The derivative of the rotation operator with respect to the angle of rotation is given by

$$\begin{aligned} \nabla_{\angle e}\dot{\mathbf{E}} &= \mathrm{E}\rfloor\mathrm{E}\exp(\angle e\,\mathrm{E}\rfloor\mathrm{E}) \\ &= \mathrm{E}\rfloor\mathrm{E}\cos\angle e + \mathrm{E}\rfloor\mathrm{E}\sin\angle e \\ &= \mathrm{E}\rfloor\mathrm{E}\dot{\mathbf{E}}, \end{aligned} \quad (3.9)$$

whose 3×3 matrix representation is given in §7. This gives a natural interpretation of the function of $\mathrm{E}\rfloor\mathrm{E}$, which otherwise seems rather abstract.

The derivatives of the rotation operator with respect to the direction of the axis of rotation are not normally needed in diffractometric goniometry, and are not discussed in this paper. However, the derivative of a rotated vector with respect to a small-angle vector representation is used in calculations of the effects of mosaicity, but an extra new notation ($\lceil\cdot\rfloor$ and $\lfloor\cdot\rceil$) is needed which will be discussed in a later paper (Thomas, 1990*b*). Although the new operators introduced in this section are derived with special reference to rotational calculations, most of them have other applications. For example, $\cdot|\cdot$ is used in calculations of X-ray beam polarization (Thomas, 1990*b*), $\cdot|\cdot$ in calculations involving detector geometry (Thomas, 1990*a*) and $\cdot\overline{|}\cdot$ in calculations of the fluorescent scattering from a foil (Thomas, 1990*a*).

4. The three-circle crystal-goniostat: (I) analytic solution

We turn now to the important practical calculation of the setting-angles of a three-circle crystal-goniostat using the notation outlined above. To avoid confusion, we distinguish here between the crystal-goniostat and the detector-goniostat on a diffractometer, so that what is conventionally called a four-circle diffractometer is in reality almost certainly a machine with a three-circle crystal-goniostat and an independent one-circle detector-goniostat. Although the following account is cast in terms of the three-circle crystal-goniostat, it is equally appropriate for any other type of goniostat. Two-circle crystal-goniostats and one-circle crystal-goniostats are included implicitly, being reduced forms in which the third axis, and the second and third axes respectively are missing; the correct working for them is to be obtained by striking out those parts which have become superfluous. Analysis of the three-circle crystal-goniostat leads to the most general setting equations capable of unique solution, and the extent to which, say, a four-circle crystal-goniostat can be characterized is left as an exercise for the reader.

The axes of a goniostat are numbered in the order that one would meet them going from the crystal to the base-

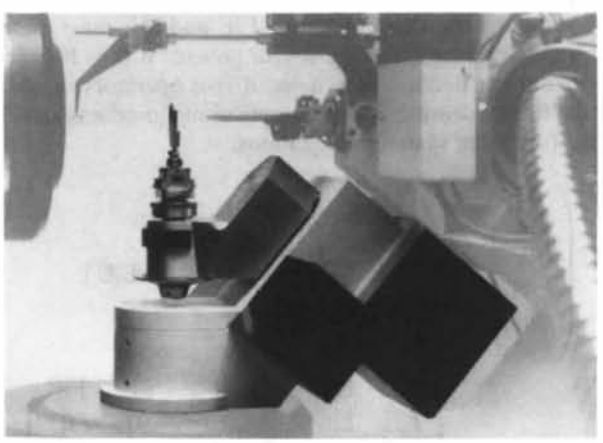

Fig. 4. The kappa-bracket goniostat of an Enraf–Nonius FAST system. The kappa axis is inclined at 50° to the vertical phi and omega axes, and the positive sense of rotation for all of the axes is clockwise as seen from above. For a long time the analysis of kappa brackets and of Eulerian cradles was handled quite differently, as if they were not related to each other. Geometrically they are entirely equivalent, and differ only in the relative orientations of their axes and in the region of orientational space accessible to them. The general equations given in §4 apply equally to all three-circle crystal-goniostats.

Table 3. *Symbol table for* §4

ε	a very small number
$\angle\kappa$	the angle of the κ axis
$\angle\omega$	the angle of the ω axis
$\angle\phi$	the angle of the ϕ axis
$\nabla_{\angle 1}, \nabla_{\angle 2}, \nabla_{\angle 3}$	operators performing differentiation with respect to goniostat angles
$\dot{\mathrm{X}}$	the chi axis of an Eulerian cradle
$\dot{\mathrm{K}}$	the kappa axis of a kappa-bracket goniostat
$\dot{\Omega}$	the omega axis both of an Eulerian cradle and of a kappa-bracket goniostat
$\dot{\Phi}$	the phi axis both of an Eulerian cradle and of a kappa-bracket goniostat
$\dot{1}$	the first goniostat axis, usually $\dot{\Phi}$
$\dot{2}$	the second goniostat axis, usually $\dot{\mathrm{X}}$ or $\dot{\mathrm{K}}$
$\dot{3}$	the third goniostat axis, usually $\dot{\Omega}$
$\angle 2_0$	the 'zero angle' of the second goniostat axis
$\dot{\mathbf{G}}$	a rotation generated by a goniostat
s_2	a constant subtrahend used in solving for $\angle 2$ in the general 321 goniostat
d_2	a constant divisor used in solving for $\angle 2$ in the general 321 goniostat
$\cos^{-1}$	the principal value of the inverse of the cosine function (result on $[0, \pi]$)
$\tan^{-1}\left\{\begin{smallmatrix} k\sin \\ k\cos \end{smallmatrix}\right\}$	the principal value of the double-argument inverse tangent function (result on $[-\pi, \pi[$)
k	a positive constant allowing the generalization of the definition of $\tan^{-1}$ and $\cot^{-1}$
$\surd$	the square root
$\sim$	can be represented by
$\leftarrow$	the computational assignment operator
$\cdot$	missing argument of a function
$[\cdot, \cdot]$	an interval closed at both extremities
$[\cdot, \cdot[$	an interval closed at the lower extremity, but open at the upper one

plate. This is convenient because it has become conventional in the analysis of the geometry of area-detector cameras and diffractometers to work as much as possible in a system in which the crystal is taken as the origin.

Thus, for a normal Eulerian cradle, $\dot{\Phi}$ is the first axis, $\dot{1}$; $\dot{\mathrm{X}}$ is the second axis, $\dot{2}$; and $\dot{\Omega}$ is the third axis, $\dot{3}$. For a kappa-bracket* goniostat as used on the Enraf–Nonius† CAD-4 diffractometer and on the Enraf–Nonius FAST system (see Fig. 4), $\dot{\Phi}$ is the first axis, $\dot{\mathrm{K}}$ is the second axis, and $\dot{\Omega}$ is the third axis. We can represent the rotation produced by the goniostat by the rotation operator (notation as in Table 3)

$$\dot{\mathbf{G}} = \dot{\mathbf{3}}\dot{\mathbf{2}}\dot{\mathbf{1}}, \tag{4.1}$$

using a natural extension of Hamilton's multiplicative‡ rule for the combination of rotations (Misner, Thorne & Wheeler, 1973, §41.1, p. 1136). The rotation that we require the goniostat to produce can be represented by another rotation operator, $\dot{\mathbf{E}}$, and therefore we wish to know the solution for the three axial angles: $\angle 1$, $\angle 2$ and $\angle 3$ when

$$\dot{\mathbf{E}} = \dot{\mathbf{G}}. \tag{4.2}$$

An axis is invariant under rotations about itself, which yields an extremely valuable eigenequation:

$$\dot{\mathbf{E}}\mathrm{E}| = \mathrm{E}|. \tag{4.3}$$

Thus, knowing that $\dot{\mathbf{E}}$ will be decomposed into the form of $\dot{\mathbf{G}}$, we can uncouple its dependence on $\angle 1$ by allowing it to act on the first axis, $\dot{1}$, or, equivalently, back-operating the first axis onto it:

$$\dot{\mathbf{E}}1| = \dot{\mathbf{3}}\dot{\mathbf{2}}\dot{\mathbf{1}}1| = \dot{\mathbf{3}}\dot{\mathbf{2}}1|. \tag{4.4}$$

It is normal to use a signed axis here, though the equation is equally true with a free one. Similarly, the operation of a sixa is also unaffected by rotation about its corresponding axis, which is represented by the reciprocal eigenequation:

$$|\mathrm{E} = |\mathrm{E}\dot{\mathbf{E}}, \tag{4.5}$$

so we are also able to uncouple the dependence of equation (4.4) on $\angle 3$ by the action of $|3$, giving

$$|3\dot{\mathbf{E}}1| = |3\dot{\mathbf{3}}\dot{\mathbf{2}}1| = |3\dot{\mathbf{2}}1|. \tag{4.6}$$

It is, equally, normal to use a signed sixa here, though the equation is also valid with a free one. This equation can be solved without knowing the internal structure of the rotation operator, $\dot{\mathbf{2}}$, in any greater detail than has already

* The kappa geometry was invented by Siem Poot of Enraf–Nonius, and was protected worldwide by patents (Poot, 1972).

† B.V. Enraf–Nonius, Röntgenweg 1, 2600 AL Delft-Holland, The Netherlands.

‡ According to Gray (1980), Lagrange gave additive formulae for infinitesimal rotations in 1788, and Rodrigues noted in 1840 that the infinitesimal motions can be integrated to give the correct form for finite rotations. But the same article makes it seem curious that the connexion was not noted more clearly by Euler, who is said to have been familiar with the products of orthogonal matrices, which he used to express successive rotations in his number-theoretical research.

been described in §3. Thus, we can expand (4.6) into the form of (2.1):

$$\begin{aligned}|3\dot{E}1| &= |3\left[2|2 + 2\overline{|}2\sin\angle 2 + 2\underline{|}2\cos\angle 2\right]1| \\ &= |32|21| + |32\overline{|}21|\sin\angle 2 + |32\underline{|}21|\cos\angle 2.\end{aligned} \tag{4.7}$$

Every goniometric equation in diffractometry, and probably everywhere else, can be cast into this form.

There are several ways to solve this equation. The simplest method, which is illustrated in Fig. 5, proceeds in two steps: we first observe that the constant factors multiplying the trigonometric functions in (4.7) can be represented as

$$|32\underline{|}21| = \sqrt{|32\overline{|}21|^2 + |32\underline{|}21|^2}\cos\angle 2_0 \tag{4.8}$$

and

$$|32\overline{|}21| = \sqrt{|32\overline{|}21|^2 + |32\underline{|}21|^2}\sin\angle 2_0, \tag{4.9}$$

where

$$\angle 2_0 = \tan^{-1}\left\{\begin{matrix}|32\overline{|}21| \\ |32\underline{|}21|\end{matrix}\right\} \equiv \tan^{-1}|3\left\{\begin{matrix}2\overline{|}2 \\ 2\underline{|}2\end{matrix}\right\}1| \tag{4.10}$$

is a scalar constant of the goniostat. Indeed, this is an angle defined without either a protractor or a metric. Equation (4.10) is the first equation which demands that a scalar magnitude can be attributed to the forms $|32\overline{|}21|$ and $|32\underline{|}21|$, though it still cannot demand that they themselves are necessarily scalar quantities, because the inverse-tangent function could itself be constructed in such a way as to make that attribution. However, in all normal representations, $|32\overline{|}21|$ and $|32\underline{|}21|$ are just real numbers. We have, of course, assumed that the square root of an operator can be taken, but this would not normally be regarded as a particularly contentious operation. Equation (4.7) then reduces to an equation containing the cosine of the difference between the solution, $\angle 2$, and $\angle 2_0$:

$$|3\dot{E}1| - |32|21| = \sqrt{|32\overline{|}21|^2 + |32\underline{|}21|^2}\cos(\angle 2 - \angle 2_0), \tag{4.11}$$

which has two possible solutions given by

$$\angle 2 = \angle 2_0 \pm \cos^{-1}\left(\frac{|3\dot{E}1| - |32|21|}{\sqrt{|32\overline{|}21|^2 + |32\underline{|}21|^2}}\right). \tag{4.12}$$

Thus we have paradoxically been able to calculate that part of the required rotation, $\dot{\mathbf{2}}$, which is most deeply embedded in the overall expression for the rotation given by (4.1) by virtue of the power of the operators |3 and 1|; whereas it might appear that that quantity in the middle of the equation would be the last to be evaluated. However, having found it, it is then an elementary matter to determine the two flanking quantities, $\dot{\mathbf{1}}$ and $\dot{\mathbf{3}}$. For steric reasons, and because of the possibility of the failure of the equations if the first axis and the third axis turn out to be parallel, we next work out the third axis, which is the one attached to the baseplate of the diffractometer. This is achieved by picking out the skew-symmetric and symmetric parts of the required rotation by matching them with those of any rotation which could be produced by the third axis acting on the known rotation of the second axis, having uncoupled the action of the first axis, and gives an immediate solution:

$$\begin{aligned}\angle 3 &= \tan^{-1}\left(\left\{\begin{matrix}3\overline{|}3 \\ 3\underline{|}3\end{matrix}\right\}\dot{2}1| \blacksquare \dot{E}1|\right) \\ &= \tan^{-1}|1\dot{E}\left\{\begin{matrix}3\overline{|}3 \\ 3\underline{|}3\end{matrix}\right\}\dot{2}1| \\ &\equiv \tan^{-1}|1\dot{2}\left\{\begin{matrix}3\overline{|}3 \\ 3\underline{|}3\end{matrix}\right\}\dot{E}1|.\end{aligned} \tag{4.13}$$

Its derivation and structure can be seen from (3.6) and (3.7) which show that $3\overline{|}3 \blacksquare \dot{\mathbf{3}} = 2\sin\angle 3$ and $3\underline{|}3 \blacksquare \dot{\mathbf{3}} = 2\cos\angle 3$, which is not invalidated when the operators are made to act on the axis, $\dot{\mathbf{2}}1|$. The rearrangement of the

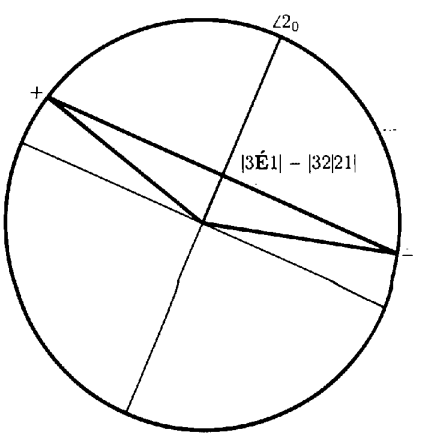

Fig. 5. The solution of equation (4.7) for $\angle 2_0$ and for the two possible values of $\angle 2$. This diagram can also be drawn as lines intersecting a sine wave, but the construction shown is simpler and exposes the nature of the angles more directly. The distance from the centre of the bold chord equals $|3\dot{E}1| - |32|21|$, and it dictates the two solutions (+ and −) for $\angle 2$. These are always symmetrically arranged about the so-called 'zero-angle', $\angle 2_0$.

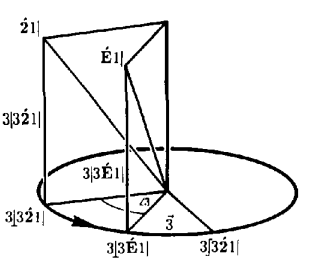

Fig. 6. The solution of equation (4.13) for $\angle 3$. The various components resulting from the expansion of equation (4.13) are displayed in the manner of the indicator diagram, Fig. 3. The term $\dot{\mathbf{E}}1|$ differs from $\dot{\mathbf{2}}\dot{\mathbf{1}}1| = \dot{\mathbf{2}}1|$ only in the application of the unknown rotation, $\dot{\mathbf{3}}$. The term $\dot{\mathbf{2}}1|$ can be regarded as a constant when solving for $\angle 3$, so much of the structure of the complete equation need not be drawn.

equation to eliminate the correspondence product makes use of the fact that the terms it separates are both axes, so the product is the same as the conventional scalar action of sixa on axis [see (3.8)]. A graphical decomposition of the equation is shown in Fig. 6.

If the action of the second-axis rotation is to bring the first axis into alignment with the third, this equation fails because all of the rotationally variant components vanish. When this happens (which it often does) the third angle can be set independently: when coded as a computer program, the value to which $\angle 3$ should be set if this equation fails is passed as an argument to the solving subroutine; the failure of (4.13) is then of little further consequence. When we come to solve the first-axis angle, we could, because of the symmetry of (4.6), write an equation exactly analogous to (4.13), in which we compare $|3\acute{E}$ with $|3\acute{2}1\rceil 1$ and $|3\acute{2}1\rfloor 1$, but this would just compound any failure to solve for the third axis with certain simultaneous failure to solve for the first. This is not a helpful outcome, since it can only be resolved by the use of another equation reserved specially for the purpose. The coding is simplified if, instead, we work out the first-axis angle by specifically undoing the (now known) rotations produced by the second and third axes, and matching with the skew-symmetric and symmetric components of rotations which could be produced by the first axis, $\acute{1}$. This is expressed by the following equation for $\angle 1$:

$$\angle 1 = \tan^{-1}\left(\left\{\begin{matrix}1\rceil 1\\ 1\rfloor 1\end{matrix}\right\} \blacksquare \grave{2}\grave{3}\acute{E}\right), \qquad (4.14)$$

which can never fail. Its structure can also be seen from (3.6) and (3.7) which show that $1\rceil 1 \blacksquare \acute{1} = 2\sin\angle 1$ and $1\rfloor 1 \blacksquare \acute{1} = 2\cos\angle 1$. As mentioned earlier, $\angle 2_0$, specified by (4.10), is a constant of the goniostat, as indeed are the subtrahend

$$s_2 = |32|21|, \qquad (4.15)$$

and the divisor

$$d_2 = \sqrt{|32\rceil 21|^2 + |32\rfloor 21|^2}, \qquad (4.16)$$

which occur in (4.12). This means that at run time, perhaps during high-speed data collection, after $\angle 2_0$, s_2 and d_2 have been calculated as constants, the complete solution of the three-circle crystal-goniostat can be expressed by just three equations [(4.12), (4.13) and (4.14)]. However, even this is not the simplest known implementation of the solution of the general case. [See §11, where (11.15) combines the function of (4.10) and (4.12) using only one inverse tangent function, and the Appendix where the close relation between the equations is given explicitly.] It turns out in practice that these equations can be coded most satisfactorily using ordinary 3×3 rotation matrices.

This solution of the three-circle crystal-goniostat in the general case has been reworked from the released computer code by Diamond (1990) using a considerably more complicated four-dimensional half-angle notation, and results in equations rather different from those used here. Diamond claims that his equation (81) reproduces (4.12) (personal communication).

5. Standard 3×3 rotation matrices

The set of 3×3 orthogonal (*i.e.* real unitary) matrices with positive determinant provide the most natural and direct computational expression of the rotation operator. Their exact form can be deduced from (3.6) without ambiguity. We first represent the (left-operating) axis by a column of three real numbers, l, m, n:

$$\mathrm{E}| \sim \begin{pmatrix} l \\ m \\ n \end{pmatrix} \equiv \frac{1}{\sqrt{1-\sigma^2}} \begin{pmatrix} \lambda \\ \mu \\ \nu \end{pmatrix}, \qquad (5.1)$$

and its conjugate (right-operating) form, or sixa, must then be a row of the same numbers:

$$|\mathrm{E} \sim (\, l \quad m \quad n\,) \equiv \frac{1}{\sqrt{1-\sigma^2}} (\, \lambda \quad \mu \quad \nu\,). \qquad (5.2)$$

The equivalent forms in Diamond's quaternion notation [$\lambda = l\sin(\angle e/2)$, $\mu = m\sin(\angle e/2)$, $\nu = n\sin(\angle e/2)$ for the vector part, and $\sigma = \cos(\angle e/2)$ for the scalar part]* are also given so that the structure of the decomposition of the half-angle form of the rotation matrix can also be seen. [See Diamond (1988), equation (7) for the full rotation, and the much less well known equation (27) for the half-rotation.] It should be noted that these numerical representations lack the generality of the operator notation upon which they are based, since they depend on the handedness and scale of the coordinate system in use.

We insist that the action of the sixa on the axis, in inner product formation, is to generate an identity operator, the scalar unit multiplier:

$$|\mathrm{EE}| \sim l^2 + m^2 + n^2 \equiv \frac{\lambda^2 + \mu^2 + \nu^2}{1-\sigma^2} = 1. \qquad (5.3)$$

With this definition, l, m, n can necessarily be interpreted as direction cosines, and this is, indeed, a common notation for them. The alternative composition, of axis acting on sixa, in outer product formation, does not produce an alternative multiplicative identity operator, but a symmetric operator specific to the line of the axis, which must

* Goldstein (1980, footnote p. 153) seems to think that these parameters should be named after Euler. However, although Euler (1775*b*) did use a tetravariate notation, it was equivalent to l, m, n and $\cos\angle e$ of the present paper, and thus did not involve half-angles. Gray (1980) points out that a half-angle tangent formalism was published first by Rodrigues in 1840, though Gauss knew of it in 1819; it would therefore still appear that Hamilton's announcements of 1843 and 1844 are the first clear accounts leading to the present-day sine–cosine half-angle formulation.

therefore be a representation of the rotationally invariant operator:

$$\begin{aligned} \mathrm{E}|\mathrm{E} &\sim \begin{pmatrix} l^2 & ml & nl \\ lm & m^2 & nm \\ ln & mn & n^2 \end{pmatrix} \\ &\equiv \frac{1}{1-\sigma^2} \begin{pmatrix} \lambda^2 & \mu\lambda & \nu\lambda \\ \lambda\mu & \mu^2 & \nu\mu \\ \lambda\nu & \mu\nu & \nu^2 \end{pmatrix}. \end{aligned} \tag{5.4}$$

Apart from an ambiguity of sign, there is only one skew-symmetric 3×3 matrix having properties satisfying the systems (3.3) and (3.7), which is

$$\begin{aligned} \mathrm{E}\underline{|}\mathrm{E} &\sim \begin{pmatrix} 0 & -n & m \\ n & 0 & -l \\ -m & l & 0 \end{pmatrix} \\ &\equiv \frac{1}{\sqrt{1-\sigma^2}} \begin{pmatrix} 0 & -\nu & \mu \\ \nu & 0 & -\lambda \\ -\mu & \lambda & 0 \end{pmatrix}, \end{aligned} \tag{5.5}$$

whose square:

$$\begin{aligned} \mathrm{E}\underline{|}\mathrm{E} &\sim \begin{pmatrix} l^2-1 & ml & nl \\ lm & m^2-1 & nm \\ ln & mn & n^2-1 \end{pmatrix} \\ &\equiv \frac{1}{1-\sigma^2} \\ &\times \begin{pmatrix} \lambda^2+\sigma^2-1 & \mu\lambda & \nu\lambda \\ \lambda\mu & \mu^2+\sigma^2-1 & \nu\mu \\ \lambda\nu & \mu\nu & \nu^2+\sigma^2-1 \end{pmatrix}, \end{aligned} \tag{5.6}$$

cube:

$$\begin{aligned} \mathrm{E}\underline{|}\mathrm{E} &\sim \begin{pmatrix} 0 & n & -m \\ -n & 0 & l \\ m & -l & 0 \end{pmatrix} \\ &\equiv \frac{1}{\sqrt{1-\sigma^2}} \begin{pmatrix} 0 & \nu & -\mu \\ -\nu & 0 & \lambda \\ \mu & -\lambda & 0 \end{pmatrix}, \end{aligned} \tag{5.7}$$

and fourth power:

$$\begin{aligned} \mathrm{E}\underline{|}\mathrm{E} &\sim \begin{pmatrix} 1-l^2 & -ml & -nl \\ -lm & 1-m^2 & -nm \\ -ln & -mn & 1-n^2 \end{pmatrix} \\ &\equiv \frac{1}{1-\sigma^2} \\ &\times \begin{pmatrix} 1-\sigma^2-\lambda^2 & -\mu\lambda & -\nu\lambda \\ -\lambda\mu & 1-\sigma^2-\mu^2 & -\nu\mu \\ -\lambda\nu & -\mu\nu & 1-\sigma^2-\nu^2 \end{pmatrix}, \end{aligned} \tag{5.8}$$

all correspond to previously specified components of rotation operators. The antisymmetries $\mathrm{E}\underline{|}\mathrm{E} = -\mathrm{E}|\mathrm{E}$ and $\mathrm{E}|\mathrm{E} = -\mathrm{E}\underline{|}\mathrm{E}$ are particularly clear in this component representation. It will be noticed that in the quaternion formalism, all of the operators contain a prefactor whose denominator vanishes for small rotations, so their numerical evaluation in that form can hardly be recommended; however, analytically they are perfectly well behaved. No such problems arise with the full-angle formalism.

The sum of rotationally invariant and symmetric operators does produce an alternative multiplicative identity element, representable by the unit matrix

$$\mathrm{E}|\mathrm{E} + \mathrm{E}\underline{|}\mathrm{E} = \mathbf{I} \sim \begin{pmatrix} 1 & 0 & 0 \\ 0 & 1 & 0 \\ 0 & 0 & 1 \end{pmatrix}, \tag{5.9}$$

whose action is readily seen from (3.6) to be the same as that of a null rotation. Indeed, this equation has already been used in the reduction of the exponential formulation of the rotation operator into the three-way split of (3.6).

With these definitions, we can reliably construct the standard 3×3 rotation matrix as

$$\begin{aligned} \acute{\mathbf{E}} &\sim \begin{pmatrix} l^2 & ml & nl \\ lm & m^2 & nm \\ ln & mn & n^2 \end{pmatrix} + \begin{pmatrix} 0 & -n & m \\ n & 0 & -l \\ -m & l & 0 \end{pmatrix} \sin\angle e \\ &+ \begin{pmatrix} 1-l^2 & -ml & -nl \\ -lm & 1-m^2 & -nm \\ -ln & -mn & 1-n^2 \end{pmatrix} \cos\angle e \\ &\equiv \frac{1}{1-\sigma^2} \begin{pmatrix} \lambda^2 & \mu\lambda & \nu\lambda \\ \lambda\mu & \mu^2 & \nu\mu \\ \lambda\nu & \mu\nu & \nu^2 \end{pmatrix} \\ &+ 2\sigma \begin{pmatrix} 0 & -\nu & \mu \\ \nu & 0 & -\lambda \\ -\mu & \lambda & 0 \end{pmatrix} \\ &+ \frac{2\sigma^2-1}{1-\sigma^2} \\ &\times \begin{pmatrix} 1-\sigma^2-\lambda^2 & -\mu\lambda & -\nu\lambda \\ -\lambda\mu & 1-\sigma^2-\mu^2 & -\nu\mu \\ -\lambda\nu & -\mu\nu & 1-\sigma^2-\nu^2 \end{pmatrix}. \end{aligned} \tag{5.10}$$

When summed, the half-angle formulation here reduces rather laboriously to the well known form [*e.g.* equation (7) in Diamond (1988), or equation (4–67) in Goldstein (1980)], in which the components of different symmetry are not clearly separated. Here, we are using $2\sigma\sqrt{1-\sigma^2}$ for $\sin\angle e$ and $2\sigma^2 - 1$ for $\cos\angle e$ which is possible since $\sigma = \cos(\angle e/2)$; this enforces consistency of notation with the standard quaternion form, in which neither the angle of rotation nor, indeed, any obvious behavioural symmetries appear.

These matrix representations assume Cartesian right-handed axes, and are therefore less general than the oper-

ator notation which does not depend on either a metric or a component representation.

Inspection of the system (3.7) shows that in a 3×3 matrix representation, the correspondence, or inner, product denoted by $\blacksquare$ is executed computationally by aligning two matrices element for element, as if laying one on top of the other, and then summing the products of overlapping, or corresponding, terms. It can therefore be computed slightly faster than the compositional product $\circ$, which becomes an ordinary matrix multiplication in this representation.

6. The three-circle crystal-goniostat: (II) iterative numerical solution

It is rather unfortunate that on an area-diffractometer the crystal-goniostat is used more often in a position where (4.13) fails than when it succeeds. This is because the phi- and omega-axes, $\dot{\Phi}$, $\dot{\Omega}$, are so often parallel. For some purposes this is of no consequence because the omega-angle, $\angle\omega$, can be set to a value which avoids collisions between the omega-block or chi-circle and the detector whilst allowing convenient access for the crystallographer. Then the phi-value, $\angle\phi$, can be determined by (4.14). If data are to be collected using the rotation method, either $\angle\omega$ or $\angle\phi$, and sometimes both in synchrony (but rarely $\angle\kappa$) will be incremented at a steady rate, so it is not necessary continually to re-evaluate the goniostat angles using the equations of the last section. However, there are occasions when it is necessary for the goniostat to be swung in a well controlled manner through the position at which $\dot{\Phi}$ becomes parallel to $\dot{\Omega}$. The most important example of this, precession motion, is presented in §9. It turns out that the method of Raphson (1690) is particularly suitable for handling this situation. Indeed, it is hardly necessary to know that we are dealing with rotations or goniostats: we need merely to apply Raphson's method mechanically in a fashion designed to drive the operator, $\acute{\mathbf{G}}$, describing the rotation produced by the goniostat into coincidence with the operator, $\acute{\mathbf{E}}$, describing the required rotation. To do this, we need to know the first derivatives (Jacobian) of $\acute{\mathbf{G}}$ with respect to the three goniostat angles. These are represented by the following three equations:

$$\nabla_{\angle 1}\acute{\mathbf{G}} = \acute{\mathbf{3}}\acute{\mathbf{2}}\left(\nabla_{\angle 1}\acute{\mathbf{1}}\right), \tag{6.1}$$

$$\nabla_{\angle 2}\acute{\mathbf{G}} = \acute{\mathbf{3}}\left(\nabla_{\angle 2}\acute{\mathbf{2}}\right)\acute{\mathbf{1}}, \tag{6.2}$$

$$\nabla_{\angle 3}\acute{\mathbf{G}} = \left(\nabla_{\angle 3}\acute{\mathbf{3}}\right)\acute{\mathbf{2}}\acute{\mathbf{1}}. \tag{6.3}$$

These equations must be calculated at the current position of the goniostat. The three derivatives are then substituted into the following equation:

$$\underbrace{\begin{pmatrix}\angle 1\\ \angle 2\\ \angle 3\end{pmatrix}}_{a'} \leftarrow \underbrace{\begin{pmatrix}\angle 1\\ \angle 2\\ \angle 3\end{pmatrix}}_{a} + \underbrace{\left[\begin{pmatrix}\nabla_{\angle 1}\acute{\mathbf{G}}\\ \nabla_{\angle 2}\acute{\mathbf{G}}\\ \nabla_{\angle 3}\acute{\mathbf{G}}\end{pmatrix} \blacksquare \left(\nabla_{\angle 1}\acute{\mathbf{G}},\ \nabla_{\angle 2}\acute{\mathbf{G}},\ \nabla_{\angle 3}\acute{\mathbf{G}}\right) + \varepsilon\mathbf{I}\right]^{-1}}_{[f'(a)]^{-1}} \begin{pmatrix}\nabla_{\angle 1}\acute{\mathbf{G}}\\ \nabla_{\angle 2}\acute{\mathbf{G}}\\ \nabla_{\angle 3}\acute{\mathbf{G}}\end{pmatrix} \blacksquare \underbrace{\left(\acute{\mathbf{E}} - \acute{\mathbf{G}}\right)}_{f(a)}. \tag{6.4}$$

which is a trivariate extension of Raphson's method. The reference comments under the braces are the standard modern notation for the method of Newton (1669) and Raphson. Formally, the product of the inverted square-matrix and the column-vector of derivatives is a generalized inverse of a row-vector of derivatives. In practice, the equation is best solved by the analytic form of the conjugate-gradient algorithm (Hestenes & Steifel, 1952; Thomas, 1989, §14), even though the square-matrix is only 3×3 positive symmetric. This is because the matrix becomes singular if any of the goniostat axes (usually $\dot{\Phi}$ and $\dot{\Omega}$) become coincident: the conjugate-gradient algorithm handles this in a very smooth fashion, dividing any incremental change equally between the aligned axes. However, although its behaviour with exact arithmetic is well defined, rounding errors can cause a perturbation when this singularity occurs, in which the differential rotations produced by the coincident axes may be ill-conditioned. This uncontrolled behaviour can be stabilized completely without materially altering the accuracy of the result by adding a very small multiple of the identity matrix, $\varepsilon\mathbf{I}$, to the matrix to be inverted. In practice, we use $\varepsilon = 0.01$.

Equation (6.4) is the preferred method of controlling a goniostat undergoing a small-angle precession motion, in which the ϕ-axis and the ω-axis are often in close alignment (see §§8 and 9).

7. The derivative of a standard rotation matrix with respect to the angle of rotation

The derivative of the rotation operator expressed as a 3×3 rotation matrix is obtained by substitution of (5.5) and (5.8) into (3.9), and is:

$$\begin{aligned}\nabla_{\angle e}\acute{\mathbf{E}} &\sim \begin{pmatrix}0 & -n & m\\ n & 0 & -l\\ -m & l & 0\end{pmatrix}\cos\angle e\\ &\quad + \begin{pmatrix}l^2-1 & ml & nl\\ lm & m^2-1 & nm\\ ln & mn & n^2-1\end{pmatrix}\sin\angle e\\ &\equiv \frac{2\sigma^2-1}{\sqrt{1-\sigma^2}}\begin{pmatrix}0 & -\nu & \mu\\ \nu & 0 & -\lambda\\ -\mu & \lambda & 0\end{pmatrix} + \frac{2\sigma}{\sqrt{1-\sigma^2}}\\ &\quad \times \begin{pmatrix}\lambda^2+\sigma^2-1 & \mu\lambda & \nu\lambda\\ \lambda\mu & \mu^2+\sigma^2-1 & \nu\mu\\ \lambda\nu & \mu\nu & \nu^2+\sigma^2-1\end{pmatrix}.\end{aligned} \tag{7.1}$$

Table 4. *Symbol table for* §8

$\dot{\mathrm{B}}$	the beam or virtual beta axis
$\|\mathrm{B}$	$\dot{\mathrm{B}}$ as a right-acting operator
$\dot{\mathrm{X}}$	the virtual chi axis
$\mathrm{X}\|\mathrm{X}$	the rotation invariant operator derived from $\dot{\mathrm{X}}$
$\mathrm{X}\overline{\|}\mathrm{X}$, $\mathrm{X}\underline{\|}\mathrm{X}$	the skew and symmetric operators derived from $\dot{\mathrm{X}}$
$\dot{\mathrm{P}}$	the virtual rho axis
$\mathrm{P}\|$	$\dot{\mathrm{P}}$ as a left-acting operator
$\mathrm{P}\overline{\|}\mathrm{P}$, $\mathrm{P}\underline{\|}\mathrm{P}$	the skew and symmetric operators derived from $\dot{\mathrm{P}}$
$\vec{\mathrm{N}}$	the normal to a reciprocal-lattice net plane to be brought into coincidence with $\dot{\mathrm{P}}$
$\|\mathrm{N}$, $\mathrm{N}\|$	$\vec{\mathrm{N}}$ as right- and left-acting operators
$\dot{\mathrm{S}}$	the swing axis
$\|\mathrm{S}$	$\dot{\mathrm{S}}$ as a right-acting operator
$\angle\rho, \angle\chi, \angle\beta$	the angles of the $\beta\chi\rho$ virtual goniostat
$\angle\beta_0$	the 'zero angle' in the solution for the third angle of the $\beta\chi\rho$ virtual goniostat
$\angle\chi_0$	the 'zero angle' in the solution for the second angle of the $\beta\chi\rho$ virtual goniostat
$\dot{\mathbf{B}}$, $\dot{\mathbf{X}}$, $\dot{\mathbf{P}}$	rotations produced by the $\beta\chi\rho$ virtual goniostat
$\dot{\mathbf{C}}$	a constrained rotation, also used as the orientation of the centre of a precession motion
d_β	a constant divisor used in solving for $\angle\beta$ in the $\beta\chi\rho$ virtual goniostat
d_χ	a constant divisor used in solving for $\angle\chi$ in the virtual $\beta\chi\rho$ goniostat
s_β	a constant subtrahend used in solving for $\angle\beta$ in the $\beta\chi\rho$ virtual goniostat
s_χ	a constant subtrahend used in solving for $\angle\chi$ in the virtual $\beta\chi\rho$ goniostat
$\mathbb{R}$	the set of real numbers
$\mathbb{Z}$	the set of whole numbers
$\longleftarrow$	becomes
$\mapsto$	a specific mapping between elements of sets
x	a general algebraic quantity
sgn	the *signum*: $\mathbb{R} \to \mathbb{Z}$; $x \mapsto \mathrm{sgn}(x)$ function: $\mathrm{sgn}(x) = 1, x > 0;\ -1, x < 0;\ 0, x = 0$
$\hat{\lambda}$	the sign of the projection of $\vec{\mathrm{N}}$ onto a signed representation of $\dot{\mathrm{P}}$
$\parallel$	is parallel to
$\wedge$	the vector cross product
$\|\cdot\|$	the absolute value

Thus the simplicity of (6.4) is somewhat deceptive; the number of machine operations to set it up and to solve it is very large. However, its behaviour is impeccable: indeed, inspection will show that there is no case of practical importance in which the trajectory of a goniostat controlled by it is ill defined. It is also rather more attractive to the computer programmer than the equations of §4 which require the sign of the second-axis angle to be evaluated carefully before attempting the solution, but it would not be appropriate to use it when the highest computational speed is required.

8. The construct of a virtual goniostat

In the previous two sections we have assumed that the crystallographic requirement could be specified by a required-orientation operator. This is not always true, and one of the most important counterexamples occurs when calculating how to bring a zone axis into alignment with the incident beam. The desire to bring a plane normal into alignment with the beam, in either the parallel or the anti-parallel sense, allows a degree of freedom, namely rotation of the crystal about the beam, which means that we cannot immediately specify the required-rotation operator, $\dot{\mathbf{E}}$. A very satisfactory resolution of this indeterminacy is achieved by inventing the construct of a 'virtual goniostat'. The idea of the virtual goniostat is to constrain the motion of the crystal to those positions that the virtual goniostat is capable of reaching. In this particular case, we invoke the use of a $\beta\chi\rho$ goniostat. The first axis, $\dot{\mathrm{P}}$ (rho) (see Table 4 for list of symbols),

$$\dot{1} \longleftarrow \dot{\mathrm{P}}, \tag{8.1}$$

is often made to correspond with the real ϕ axis, and can be in any orientation which is not parallel to the incident beam. The second axis, $\dot{\mathrm{X}}$ (chi), is defined to be perpendicular both to $\dot{\mathrm{P}}$ and to the beam, $\dot{\mathrm{B}}$:

$$\dot{2} \longleftarrow \dot{\mathrm{X}} \parallel \dot{\mathrm{B}} \wedge \dot{\mathrm{P}}. \tag{8.2}$$

and the third axis is $\dot{\mathrm{B}}$ (beta), defined to be parallel to the beam:

$$\dot{3} \longleftarrow \dot{\mathrm{B}}. \tag{8.3}$$

This definition of the $\beta\chi\rho$ goniostat guarantees that the ρ axis, $\dot{\mathrm{P}}$, can be brought into alignment with the beam, or β axis. If we were to spin the ρ axis, the plane normal, $\vec{\mathrm{N}}$, which is required to be brought into coincidence with

the beam, would sweep out a cone, and the cosine of the semi-angle would be

$$\big||\mathrm{NP}|\big| = \hat{\lambda}|\mathrm{NP}|, \tag{8.4}$$

where the scalar constant, $\hat{\lambda}$, determines whether the plane normal is aligned in a parallel or anti-parallel sense with respect to a signed representation of the ρ axis:

$$\hat{\lambda} = \mathrm{sgn}|\mathrm{NP}|. \tag{8.5}$$

The first step to bring the plane normal into coincidence with the beam is to rotate the virtual χ circle so that the ρ axis subtends the same angle to the beam axis as it does to the normal of the plane to be observed. This can be done by setting the two cosines equal:

$$\big||\mathrm{NP}|\big| = |\mathrm{B}\dot{\mathbf{X}}\mathrm{P}|. \tag{8.6}$$

The sign of the the cosine term, $|\mathrm{NP}|$, is immaterial here, since the plane can be aligned with the beam in either orientation, but on a real diffractometer we may choose the sign of $|\mathrm{B}\dot{\mathbf{X}}\mathrm{P}|$, which is the cosine of the angle between the ρ axis and the beam. On the FAST system, this is usually chosen to be positive, as reflected by (8.6). Equation (8.6) has the same form as (4.6) and its solution follows the same route. We define the constant subtrahend of the virtual goniostat as

$$s_\chi = |\mathrm{BX}|\mathrm{XP}|, \tag{8.7}$$

the constant divisor of the virtual goniostat as

$$d_\chi = \sqrt{|\mathrm{BX}\rceil\mathrm{XP}|^2 + |\mathrm{BX}\lfloor\mathrm{XP}|^2}, \tag{8.8}$$

and the zero-angle of the second axis of the virtual goniostat as

$$\angle\chi_0 = \tan^{-1}|\mathrm{B}\left\{\begin{matrix}\mathrm{X}\rceil\mathrm{X}\\ \mathrm{X}\lfloor\mathrm{X}\end{matrix}\right\}\mathrm{P}|. \tag{8.9}$$

This allows us to evaluate the setting of $\angle\chi$ which would bring the plane normal into alignment with the beam as

$$\angle\chi = \left[\begin{matrix}\\ -\pi\end{matrix}\right. \angle\chi_0 \pm \cos^{-1}\left(\frac{\big||\mathrm{NP}|\big| - s_\chi}{d_\chi}\right) \left.\begin{matrix}\\ \pi\end{matrix}\right[, \tag{8.10}$$

where the choice of plus or minus is made so that we get a value of $\angle\chi$ which does not cause the goniostat to collide with the detector. In practice, on the FAST system, with the normal definitions, this would mean that $\angle\chi$ would be negative. In addition, the value of $\angle\chi$ is constrained to lie on the interval $[-\pi, \pi[$. The range of $\angle\chi$ values which can be achieved on a real diffractometer is somewhat limited, because the goniometer head will ultimately foul the collimator, backstop or the detector. On the FAST system, we can accept a value of $\angle\chi$ as low as $-63°$ before any problems arise, so there is a cone of semi-angle 27° with respect to the crystal containing normals to planes which cannot be observed. This restriction is acceptable in practice because the geometry of planes whose normals lie within this cone can always be examined implicitly, but reliably, by examining principal planes whose normals lie within $\sin^{-1}\sqrt{2/3} \sim 55°$ of the ρ axis [see Thomas (1982*a*), §5.3.3, p. (5.9)]. Once $\angle\chi$ has been set, we can bring the plane normal into alignment with the beam merely by rotating the ρ axis. Once the rotation operator, $\dot{\mathbf{X}}$, has been evaluated, both the sine and the cosine of the required $\angle\rho$ setting are available, as given by the following formulae, which are derived by considering the geometry of the plane normal to the ρ axis:

$$\sin\angle\rho = \frac{\hat{\lambda}|\mathrm{B}\dot{\mathbf{X}}\mathrm{P}\rceil\mathrm{PN}|}{|\mathrm{NP}\rceil\mathrm{PN}|}, \tag{8.11}$$

$$\cos\angle\rho = \frac{\hat{\lambda}|\mathrm{B}\dot{\mathbf{X}}\mathrm{P}\lfloor\mathrm{PN}|}{|\mathrm{NP}\rceil\mathrm{PN}|}. \tag{8.12}$$

However, in practice, the denominator of these equations need not be used, and indeed, it can only cause trouble by vanishing in the event that $\vec{\mathrm{N}}$ is parallel to $\dot{\mathrm{P}}$. (The numerators also vanish.) We use, as always, the double-argument inverse of the tangent function to obtain

$$\angle\rho = \tan^{-1}\hat{\lambda}|\mathrm{B}\dot{\mathbf{X}}\left\{\begin{matrix}\mathrm{P}\rceil\mathrm{P}\\ \mathrm{P}\lfloor\mathrm{P}\end{matrix}\right\}\mathrm{N}|. \tag{8.13}$$

This equation also fails if $\vec{\mathrm{N}}$ is parallel to $\dot{\mathrm{P}}$, but this is of no consequence, and providing that there are no wires or tubes attached to a crystal-cooler preventing free motion of the goniometer-head, any solution is equally acceptable if $\dot{\mathrm{P}}$ corresponds with the real $\dot{\Phi}$. We already know the χ-rotation operator, $\dot{\mathbf{X}}$, and we can then demand that the rotated position of the ρ axis, $\dot{\mathbf{X}}\mathrm{P}|$, be perpendicular to an axis which we shall call the swing axis, $\dot{\mathrm{S}}$, which is usually made to correspond with the optic axis of the crystal-viewing telescope. This has the effect of constraining the virtual χ axis to lie along the telescope axis, which makes $\dot{\mathrm{S}}$ perpendicular to $\dot{\mathrm{P}}$. The equation which must be satisfied is

$$|\mathrm{S}\dot{\mathrm{B}}\dot{\mathbf{X}}\mathrm{P}| = 0. \tag{8.14}$$

This, again, has the same form as (4.6), but we would not normally regard either the swing axis, $\dot{\mathrm{S}}$, or the rotated ρ axis, $\dot{\mathbf{X}}\mathrm{P}|$, as goniostat axes. Even so, the solution follows the normal pattern where we define a subtrahend

$$s_\beta = |\mathrm{SB}|\mathrm{B}\dot{\mathbf{X}}\mathrm{P}|, \tag{8.15}$$

a divisor

$$d_\beta = \sqrt{|\mathrm{SB}\rceil\mathrm{B}\dot{\mathbf{X}}\mathrm{P}|^2 + |\mathrm{SB}\lfloor\mathrm{B}\dot{\mathbf{X}}\mathrm{P}|^2}, \tag{8.16}$$

a zero angle, this time about the beam axis,

$$\angle\beta_0 = \tan^{-1}|\mathrm{S}\left\{\begin{matrix}\mathrm{B}\rceil\mathrm{B}\\ \mathrm{B}\lfloor\mathrm{B}\end{matrix}\right\}\dot{\mathbf{X}}\mathrm{P}|, \tag{8.17}$$

and finally the beta angle itself

$$\angle\beta = \left[\begin{matrix}\\ -\pi\end{matrix}\right. \angle\beta_0 \pm \cos^{-1}\left(\frac{-s_\beta}{d_\beta}\right) \left.\begin{matrix}\\ \pi\end{matrix}\right[, \tag{8.18}$$

Table 5. *Symbol table for* §9

$\acute{\mathbf{c}}$, $\acute{\mathbf{s}}$	a pair of small-angle rotations used as generators of a general precession motion
$\angle o$	an instantaneous (*i.e.* not necessarily constant) precession angle
$\acute{\mathbf{o}}$	a small-angle rotation describing a precession motion
$\acute{\mathbf{O}}$	an ordinary rotation operator equivalent to $\acute{\mathbf{o}}$
$\check{\mathbf{o}}$	a small-angle vector = ($\check{\lambda}$, $\check{\mu}$, $\check{\nu}$) representing $\acute{\mathbf{o}}$; its direction of action is denoted by angle brackets
$\angle\vartheta$	an angular parameter describing the development of a precession motion
$\Longleftrightarrow$	implies and is implied by
$\|\| \cdot \|\|$	the Euclidean norm of a vector or covector

which is normally a constant. The solutions for the three angles, $\angle\beta$, $\angle\chi$, and $\angle\rho$, are used to specify a constrained-rotation operator

$$\acute{\mathbf{C}} = \acute{\mathbf{B}}\acute{\mathbf{X}}\acute{\mathbf{P}}, \tag{8.19}$$

uniquely. We are now in a position to solve for the angles of the real goniostat, $\angle 1$, $\angle 2$ and $\angle 3$, using (4.12)–(4.14), and can choose the sign of the second axis to avoid steric problems. On the FAST system, the only problem of importance is the necessity to avoid a collision of the crystal-goniostat with the crystal-viewing telescope, and the more negative solution for $\angle\beta$ is always chosen.

9. Precession motions and a vector notation for small-angle rotations

It is very convenient on an area-detector diffractometer to be able to perform a precession motion after aligning the normal of a reciprocal-lattice net plane (*i.e.* zone axis) with the incident beam. This results in a characteristic photograph which can be used for alignment and crystal-assessment purposes. The same motion is also valuable when using a fluorescent scatterer to calibrate the response of an area diffractometer (Thomas, 1989, 1990*a*). The mean orientation of the crystal, $\acute{\mathbf{C}}$, during these motions is calculated according to the equations of §8.

To generate a precession motion, we combine rotations as if vectorially according to

$$\acute{\mathbf{o}} = \acute{\mathbf{s}}\sin\angle\vartheta + \acute{\mathbf{c}}\cos\angle\vartheta, \tag{9.1}$$

where $\angle\vartheta$ is a parameter controlling the evolution of the precession motion (Table 5 for notation). The rotations denoted vectorially by $\acute{\mathbf{s}}$ and $\acute{\mathbf{c}}$ need bear no special relationship to each other, but generally they are set to be of the same magnitude, and to act about orthogonal axes mutually perpendicular to the incident beam. In such a case, $\angle o$ (defined below) becomes constant and equivalent to Buerger's angle, $\bar{\mu}$. The vectorial addition implicit in (9.1) works even when the angles of rotation are not very small, as demonstrated in Fig. 1, where the axis, $\dot{\mathrm{o}}$, of the resulting rotation is at the zenith, and both $\angle c$ and $\angle s$ are rather large. Neither $\acute{\mathbf{s}}$ nor $\acute{\mathbf{c}}$ is held to act first in (9.1): they act simultaneously, obviating the problems noted by Rodrigues (1840) of non-commutativity with respect to the axis (but not the magnitude) of the resulting rotation.

It should be noted that whereas $\acute{\mathbf{s}}$, $\acute{\mathbf{c}}$ and $\acute{\mathbf{o}}$ do represent rotations, they do not act as operators, and, in practice, we represent these rotations by small-angle vectors such as

$$\acute{\mathbf{o}} \sim \check{\mathbf{o}}\rangle \equiv \begin{pmatrix} \check{\lambda} \\ \check{\mu} \\ \check{\nu} \end{pmatrix} \quad \Longleftrightarrow \quad \langle\check{\mathbf{o}} \equiv (\,\check{\lambda}, \check{\mu}, \check{\nu}\,), \tag{9.2}$$

whose components, apart from a factor of two, correspond with the first three components, λ, μ, ν, of the four-dimensional real notation recommended by Diamond (1988) when the square of the angle of rotation is negligible. In the computer programs developed for the Enraf–Nonius FAST system in Cambridge, so-called vectors like those in (9.2) are used extensively for internal communication of rotations.

Small-angle vector representations of rotations can be converted into general representations of rotation through the intermediary forms of the signed axis and angle of rotation:

$$\angle o = \|\check{\mathbf{o}}\|, \tag{9.3}$$

$$\vec{\mathrm{O}} = \check{\mathbf{o}}/\angle o. \tag{9.4}$$

Then $\acute{\mathbf{O}} = \acute{\mathbf{O}}(\vec{\mathrm{O}}, \angle o)$ can be generated in the normal way. The notation of (9.2) in conjunction with (9.3) and (9.4) is useful for basic work with rotations of any magnitude, providing that a well behaved differential structure is not needed.

The calculation of a precession motion is completed by operating $\acute{\mathbf{O}}(\equiv \acute{\mathbf{o}})$ onto $\acute{\mathbf{C}}$ to give

$$\acute{\mathbf{E}} = \acute{\mathbf{O}}\acute{\mathbf{C}}, \tag{9.5}$$

and solving using the iterative equations of §6. It will be noticed that the motion represented by $\acute{\mathbf{O}}$ or by $\acute{\mathbf{E}}$ is a genuine precession, and a well made three-circle goniostat driven in accordance with (9.5) will execute a large-angle precession motion more accurately than can a Buerger precession camera, which has only two-circle supporting cradles (Buerger, 1944, 1960).

10. Crystal-viewing positions

On a diffractometer which has an Eulerian cradle to support the crystal, there is usually no difficulty in setting up standard viewing positions to aid positional adjustments of the crystal on the goniometer-head. This is not true

Table 6. *Symbol table for* §10

$\mathbb{R}^3$	the vector space spanned by ordered triplets of real numbers
$\mathbf{H}$	the adjustment axes of a goniometer-head, arranged as a matrix
$\vec{H}_U, \vec{H}_V, \vec{H}_W$	the adjustment axes of a goniometer-head, assumed mutually perpendicular
$\mathbf{T}$	the axes of the crystal viewing telescope, arranged as a matrix
$\vec{T}_U, \vec{T}_O, \vec{T}_W$	the optic axis (O) and the two cross-wire axes (U and W) of the crystal viewing telescope
$\acute{\mathrm{V}}$	a rotation operator specifying a standard crystal viewing position relative to the telescope
$\acute{V}$	components of $\acute{\mathrm{V}}$ in its representation as a 3×3 rotation matrix

with a kappa-bracket diffractometer for steric reasons, and it is generally more helpful to make use of a small computer program which can make use of a table of useful viewing orientations held in a convenient form. To do this, we define a quantity, $\mathbf{H}$ (Table 6), which describes the orientation of the slides on the goniometer-head. A suitable representation for it is

$$\mathbf{H}\cdot \sim \left(\vec{H}_U \quad \vec{H}_V \quad \vec{H}_W\right), \tag{10.1}$$

where $\vec{H}_U$, $\vec{H}_V$ and $\vec{H}_W$ point along the three slides in the direction conventionally taken as positive. We similarly define a quantity, $\mathbf{T}$, to describe the three axes of the crystal-viewing telescope, equally well represented by a triplet of pointers

$$\mathbf{T}\cdot \sim \left(\vec{T}_U \quad \vec{T}_O \quad \vec{T}_W\right). \tag{10.2}$$

It would be normal for both sets of pointers to form a mutually orthogonal right-handed triplet, and since no meaning can be attached to their length, they can be set to be 'unit vectors' for algebraic convenience, so that

$$\mathbf{H}\cdot\mathbf{H} = \mathbf{I} \tag{10.3}$$

and

$$\mathbf{T}\cdot\mathbf{T} = \mathbf{I}, \tag{10.4}$$

at which point the computational behaviour of the pointers in $\mathbf{H}$ and in $\mathbf{T}$ becomes so similar to that of signed axes that we can even adopt a matching notation. In these equations the centred dot is used to denote the direction of action of $\mathbf{H}$ and $\mathbf{T}$ when used as operators. Computationally, moving the dot from right to left is equivalent to transposing the matrix. Acting as operators, $\cdot\mathbf{H}$ and $\cdot\mathbf{T}$ map $\mathbb{E}^3$, as a model of direct or reciprocal space, to the vector space, $\mathbb{R}^3$; thus $\mathbf{H}\cdot$ and $\mathbf{T}\cdot$ map $\mathbb{R}^3$ into $\mathbb{E}^3$, whilst 3×3 rotation matrices map $\mathbb{R}^3$ into itself. The rotation operator, $\acute{\mathbf{E}}$, characterizing the required motion of the goniostat is also held to act autonomically, mapping $\mathbb{E}^3$ into itself. When viewing the crystal, we require that the goniometer-head axes, $\mathbf{H}$, be reorientated by the goniostat to bring them into some standard relative alignment with the telescope, chosen to facilitate the adjustment of the slides. Given the action of the operators, and that we wish to rotate the goniometer-head rather than the telescope, there is only one possible equation to represent this, which is:

$$\begin{aligned}\acute{\mathbf{E}} &= \mathbf{T}\cdot\acute{\mathrm{V}}_n\cdot\mathbf{H}\\ &\sim \left(\vec{T}_U| \quad \vec{T}_O| \quad \vec{T}_W|\right)\cdot\\ &\quad\begin{pmatrix}\acute{V}_{nUU} & \acute{V}_{nUV} & \acute{V}_{nUW}\\ \acute{V}_{nOU} & \acute{V}_{nOV} & \acute{V}_{nOW}\\ \acute{V}_{nWU} & \acute{V}_{nWV} & \acute{V}_{nWW}\end{pmatrix}\cdot\begin{pmatrix}|\vec{H}_U\\ |\vec{H}_V\\ |\vec{H}_W\end{pmatrix}.\end{aligned} \tag{10.5}$$

The structure of this equation forces $\acute{\mathrm{V}}_n$, the representation of the 'nth standard view', to be an archetypal 3×3 rotation matrix. Inspection of (10.5) will show that if the unit matrix substitutes for $\acute{\mathrm{V}}$, then $\acute{\mathbf{E}}$ does, indeed, request a motion which brings the head axes into alignment with the telescope axes, as illustrated in Fig. 7.

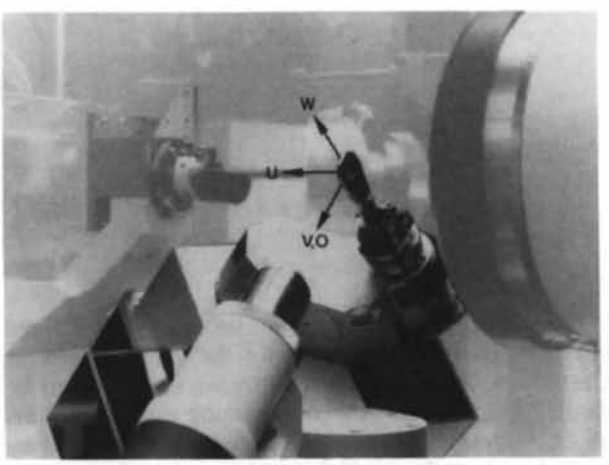

Fig. 7. The viewing position, V_{U+}. The calculations of the viewing positions are cast in such a way that the rotation matrices representing them bear a simple relationship to the view the experimenter obtains by looking down the crystal telescope. The view shown is the datum position, when no rotation is requested. The geometry of the FAST system means that the horizontal slides can be adjusted simply by flipping the goniometer-head through 180° repeatedly for each of the perpendicular slides. This means that the first four standard viewing positions are represented by particularly simple rotation matrices. However, it is not possible to rotate the goniometer-head through 180° about any axis suitable for adjusting the vertical jack without causing a collision with other parts of the hardware. For this reason, we adopt the tactic of swinging the goniometer-head to plus or minus 45° about the optic axis of the telescope, and the crystallographer can gauge the position of the centre of rotation against the telescope cross wires.

Table 7. *Standard-view matrices for the Enraf–Nonius FAST system*

The sign subscripted to each rotation matrix specifies which solution for $\angle\kappa$ is to be used. $\acute{V}_{U+}$ and $\acute{V}_{U-}$ are used to adjust the U slide of the goniometer-head. $\acute{V}_{V+}$ and $\acute{V}_{V-}$ are used similarly to adjust the V slide. $\acute{V}_{Wlx}$ and $\acute{V}_{Wrx}$ or $\acute{V}_{Wly}$ and $\acute{V}_{Wry}$ are used to adjust the W jack. $\acute{V}_{QUIT}$ is used to park the goniostat safely after the crystal is centred. The symbols x, y, z, U, V, W and O on the last three matrices are labels identifying the elements.

$$\acute{V}_{U+} = \begin{pmatrix} 1 & 0 & 0 \\ 0 & 1 & 0 \\ 0 & 0 & 1 \end{pmatrix}_- \qquad \acute{V}_{U-} = \begin{pmatrix} -1 & 0 & 0 \\ 0 & -1 & 0 \\ 0 & 0 & 1 \end{pmatrix}_-$$

$$\acute{V}_{V+} = \begin{pmatrix} 0 & -1 & 0 \\ 1 & 0 & 0 \\ 0 & 0 & 1 \end{pmatrix}_- \qquad \acute{V}_{V-} = \begin{pmatrix} 0 & 1 & 0 \\ -1 & 0 & 0 \\ 0 & 0 & 1 \end{pmatrix}_-$$

$$\acute{V}_{Wlx} = \begin{pmatrix} 0 & \frac{-1}{\sqrt{2}} & \frac{-1}{\sqrt{2}} \\ 1 & 0 & 0 \\ 0 & \frac{-1}{\sqrt{2}} & \frac{1}{\sqrt{2}} \end{pmatrix}_+ \qquad \acute{V}_{Wrx} = \begin{pmatrix} 0 & \frac{-1}{\sqrt{2}} & \frac{1}{\sqrt{2}} \\ 1 & 0 & 0 \\ 0 & \frac{1}{\sqrt{2}} & \frac{1}{\sqrt{2}} \end{pmatrix}_-$$

$$\acute{V}_{Wly} = \begin{pmatrix} \frac{1}{\sqrt{2}} & 0 & \frac{-1}{\sqrt{2}} \\ 0 & 1 & 0 \\ \frac{1}{\sqrt{2}} & 0 & \frac{1}{\sqrt{2}} \end{pmatrix}_+ \qquad \acute{V}_{Wry} = \begin{pmatrix} \frac{1}{\sqrt{2}} & 0 & \frac{1}{\sqrt{2}} \\ 0 & 1 & 0 \\ \frac{-1}{\sqrt{2}} & 0 & \frac{1}{\sqrt{2}} \end{pmatrix}_-$$

$$\acute{V}_{QUIT} = \begin{array}{c} \\ x \\ y \\ z \end{array} \begin{array}{c} \begin{array}{ccc} x & y & z \end{array} \\ \begin{pmatrix} 1 & 0 & 0 \\ 0 & 1 & 0 \\ 0 & 0 & 1 \end{pmatrix}_- \end{array}$$

$$\mathbf{T}\cdot \sim \begin{array}{c} \\ x \\ y \\ z \end{array} \begin{array}{c} \begin{array}{ccc} U & O & W \end{array} \\ \begin{pmatrix} 1 & 0 & 0 \\ 0 & \frac{1}{\sqrt{2}} & \frac{1}{\sqrt{2}} \\ 0 & \frac{-1}{\sqrt{2}} & \frac{1}{\sqrt{2}} \end{pmatrix} \end{array} \qquad \mathbf{H}\cdot \sim \begin{array}{c} \\ x \\ y \\ z \end{array} \begin{array}{c} \begin{array}{ccc} U & V & W \end{array} \\ \begin{pmatrix} 1 & 0 & 0 \\ 0 & 1 & 0 \\ 0 & 0 & 1 \end{pmatrix} \end{array}$$

Equation (10.5) has been used for many years in the computer program developed for the FAST system at Cambridge, and eight standard views are found to be ample. The matrices, $\acute{V}_n$, representing simple rotations about the telescope axes were originally calculated by hand, based on the positions of the goniostat which are sterically allowable, but this is much simpler than calculating axial angles directly when the kappa axis is inclined at about 50° to the omega and phi axes. They are shown explicitly in Table 7. The values of the components of the matrices representing the goniometer-head and the telescope are those for a standard FAST system using the preferred laboratory axes (x towards the source, y towards the front of the machine and z upwards).

11. The diffraction angle

The diffraction condition for X-rays is defined by momentum balance and energy balance. A convenient form to represent both the crystal momentum and the momenta of the incident and scattered photons is to use operators. These may be left- or right-acting, and in momentum space (and therefore in reciprocal space) they behave like vectors. Computationally, they can be represented by column or row vectors respectively. Thus, in the absence of phonon coupling, we can write (see Table 8 for notation)

$$\langle \mathrm{T} = \langle \mathrm{R} - \langle \mathrm{S} \iff \mathrm{T}\rangle = \mathrm{R}\rangle - \mathrm{S}\rangle, \qquad (11.1)$$

where $-\mathrm{S}\rangle$ represents the momentum of the incident photon, $\mathrm{T}\rangle$ represents the momentum of the scattered photon, and $\mathrm{R}\rangle$, which represents the crystal momentum, is often referred to as a reciprocal-lattice vector. The energy of a photon is conventionally given by $E = cp = c\hbar\|\mathrm{k}\|$, but the most convenient way of expressing the conservation of energy here is by means of a quadratic form proportional to E^2:

$$\langle \mathrm{TT}\rangle = \langle \mathrm{SS}\rangle. \qquad (11.2)$$

Table 8. *Symbol table for* §11

c	the speed of light
E	the energy of a photon
p	modulus of momentum
k	a wavevector
R⟩, ⟨R	the periodic structure of a Bragg-plane in the diffracting position, and its conjugate
S⟩, ⟨S	the periodic structure of minus the (mean) incident beam wavevector, and its conjugate
T⟩, ⟨T	the periodic structure of the scattered beam wavevector, and its conjugate
X⟩, ⟨X	the periodic structure of a Bragg-plane (referred to the crystal frame) and its conjugate
$\angle\tau$	an angle which is used when $\angle\psi$ cannot be defined
$\angle\psi$	the (Arndt–Wonacott) diffraction angle
$\dot{\Psi}$, $\dot{\Psi}$	rotation through $\angle\psi$, and its inverse
$\Psi\|\Psi$	the diffraction-angle invariant operator
$\Psi\rceil\Psi$, $\Psi\lceil\Psi$	the diffraction-angle skew-symmetric operator, and its inverse
$\Psi\lfloor\Psi$	the diffraction-angle symmetric operator
$\nabla_{\angle\psi}$	the derivative with respect to $\angle\psi$
ϵ	the symmetric form $\langle S\Psi\lfloor\Psi X\rangle = \langle X\Psi\lfloor\Psi S\rangle$
η	the antisymmetric form $\langle S\Psi\rceil\Psi X\rangle = \langle X\Psi\lceil\Psi S\rangle = -\langle X\Psi\rceil\Psi S\rangle = -\langle S\Psi\lceil\Psi X\rangle$
ρ	the symmetric form $\langle S\Psi\lfloor\Psi R\rangle = \langle R\Psi\lfloor\Psi S\rangle$
x	a general parameter
y	the antisymmetric form $\langle S\Psi\rceil\Psi R\rangle = \langle R\Psi\lceil\Psi S\rangle = -\langle R\Psi\rceil\Psi S\rangle = -\langle S\Psi\lceil\Psi R\rangle$
cot	the cotangent function
$\cot^{-1}\left\{\begin{matrix}k\cos\\k\sin\end{matrix}\right\}$	the double-argument inverse of the cotangent function

The symmetry of the notation used here, even more strongly reminiscent of the 'bra-ket' notation of Dirac (1958), enables the symmetry of scalar forms such as those in (11.2) to be identified immediately. The direction of action of the symbols follows the same convention as that for axes and sixas in §4: the naked side of the symbol displays the geometrical properties, and the marked side displays only scalar properties. The scalar form $\langle SR\rangle = \langle RS\rangle$ is symmetric, so these two equations can be combined by substitution of (11.1) into (11.2) to give the equation known as 'the diffraction condition':

$$\begin{aligned}\langle RR\rangle - \langle SR\rangle - \langle RS\rangle &\equiv \langle RR\rangle - 2\langle RS\rangle\\ &\equiv \langle RR\rangle - 2\langle SR\rangle\\ &= 0.\end{aligned} \tag{11.3}$$

If R⟩ is taken as the argument, this is the equation of the Ewald sphere; and if S⟩ is taken as the argument, it is the equation of the diffraction plane. We define the (Arndt–Wonacott) diffraction angle, $\angle\psi$, as the angle through which the crystal must be turned about the rotation axis in order that the Bragg plane represented by X⟩ when the goniostat is at its datum position be brought into the diffracting position, when it will be represented by R⟩. The corresponding rotation is denoted by $\dot{\Psi}$, and therefore

$$R\rangle = \dot{\Psi}X\rangle \iff \langle R = \langle X\dot{\Psi}. \tag{11.4}$$

Substitution of this into (11.3) gives directly

$$\langle X\dot{\Psi}\dot{\Psi}X\rangle - 2\langle S\dot{\Psi}X\rangle = 0, \tag{11.5}$$

but this reduces trivially to

$$\frac{\langle XX\rangle}{2} - \langle S\dot{\Psi}X\rangle = 0, \tag{11.6}$$

because $\dot{\Psi}\dot{\Psi} \equiv \mathbf{I}$ cancels out. We can then expand $\dot{\Psi}$ using (3.6) so that (11.6) becomes*

$$\frac{\langle XX\rangle}{2} - \langle S\Psi|\Psi X\rangle - \langle S\Psi\rceil\Psi X\rangle \sin\angle\psi - \langle S\Psi\lfloor\Psi X\rangle \cos\angle\psi = 0. \tag{11.7}$$

This equation also has the same form as the fundamental goniometric equation (4.7) even though there are no first- or third-axis angles. Solving by the normal route for the second axis angle would give

$$\begin{aligned}\angle\psi = \tan^{-1}\langle S\left\{\begin{matrix}\Psi\rceil\Psi\\ \Psi\lfloor\Psi\end{matrix}\right\}X\rangle\\ \pm\cos^{-1}\left(\frac{\langle XX\rangle/2 - \langle S\Psi|\Psi X\rangle}{\sqrt{\langle S\Psi\rceil\Psi X\rangle^2 + \langle S\Psi\lfloor\Psi X\rangle^2}}\right),\end{aligned} \tag{11.8}$$

which is the generalized form of the dimensionless equation (7.13) in Wonacott (1977). However, an alternative solution involving only one inverse trigonometric

* Note that the equivalent formulae given by Bricogne (1986, bottom of p. 110) are correct only for the normal-beam geometry, since they omit the $\langle S\Psi|\Psi X\rangle$ term. Messerschmidt's (1986, p. 64) formula has a peculiar structure, missing *three* terms, and is correct only when the basis vectors of his representation are tied (rather undesirably) both to the rotation axis and to the reciprocal-lattice vector in such a way that the missing terms are forced to vanish.

calculation is usually preferred in practice, particularly when predicting the positions of diffraction spots at high speed during dynamic 'diffractometer mode' data collection (Thomas, 1982*a*, *b*, 1985). We can define the skew-symmetric form

$$\eta = \langle \mathrm{S}\Psi\rfloor\Psi\mathrm{X}\rangle, \tag{11.9}$$

and the symmetric form

$$\epsilon = \langle \mathrm{S}\Psi\lfloor\Psi\mathrm{X}\rangle. \tag{11.10}$$

We also define, somewhat less obviously, the skew-symmetric form

$$\begin{aligned} y = \langle \mathrm{S}\Psi\rfloor\Psi\mathrm{R}\rangle &= \langle \mathrm{S}\Psi\rfloor\Psi\dot{\Psi}\mathrm{X}\rangle \\ &= \langle \mathrm{S}\Psi\rfloor\Psi\mathrm{X}\rangle\cos\angle\psi - \langle \mathrm{S}\Psi\lfloor\Psi\mathrm{X}\rangle\sin\angle\psi \\ &= \langle \mathrm{S}\nabla_{\angle\psi}\dot{\Psi}\mathrm{X}\rangle \\ &= \langle \mathrm{S}\nabla_{\angle\psi}\mathrm{R}\rangle, \end{aligned} \tag{11.11}$$

which is what η would have been if X⟩ were in the diffracting position, and the symmetric form

$$\begin{aligned} \rho = \langle \mathrm{S}\Psi\lfloor\Psi\mathrm{R}\rangle &= \langle \mathrm{S}\Psi\lfloor\Psi\dot{\Psi}\mathrm{X}\rangle \\ &= \langle \mathrm{S}\Psi\rfloor\Psi\mathrm{X}\rangle\sin\angle\psi + \langle \mathrm{S}\Psi\lfloor\Psi\mathrm{X}\rangle\cos\angle\psi \\ &= \frac{\langle \mathrm{XX}\rangle}{2} - \langle \mathrm{S}\Psi|\Psi\mathrm{X}\rangle, \end{aligned} \tag{11.12}$$

which is what ϵ would have been if X⟩ were in the diffracting position. [*Cf.* equations (3.3), (3.6) and (3.9).] The skew-symmetric form, y, is immediately recognisable as being proportional to the instantaneous signed inverse Lorentz factor whenever $\dot{\Psi}$ represents the instantaneous rotation axis [see Milch & Minor (1974), equation (7); Wonacott (1977), §7.3.5, equation (7.35) or Thomas (1982*a*), §2.2.2, p. (2.4)] and satisfies

$$\xi^2 \propto y^2 + \rho^2 = \eta^2 + \epsilon^2 \iff y = \pm\sqrt{\eta^2 + \epsilon^2 - \rho^2}, \tag{11.13}$$

where ξ is equivalent in function to the same symbol conventionally used dimensionlessly in the rotation method. The latter equation is a generalized form of that quoted by Lipson (1972): $L^{-1} = (\sin^2 2\theta - \zeta^2)^{1/2}$. Then substituting $2\tan(\angle\psi/2)/[1 + \tan^2(\angle\psi/2)]$ for $\sin\angle\psi$ and $[1 - \tan^2(\angle\psi/2)]/[1 + \tan^2(\angle\psi/2)]$ for $\cos\angle\psi$, (11.7) becomes

$$(\rho + \epsilon)\tan^2\frac{\angle\psi}{2} - 2\eta\tan\frac{\angle\psi}{2} + \rho - \epsilon = 0, \tag{11.14}$$

whose solution [with the form of y given in (11.13)] is given by

$$\begin{aligned} \angle\psi &= 2\tan^{-1}\left\{\begin{matrix}\eta - y\\ \epsilon + \rho\end{matrix}\right\} \\ &= 2\tan^{-1}\left\{\begin{matrix}\langle \mathrm{S}\Psi\rfloor\Psi\mathrm{X}\rangle - \langle \mathrm{S}\Psi\rfloor\Psi\mathrm{R}\rangle\\ \langle \mathrm{S}\Psi\lfloor\Psi\mathrm{X}\rangle + \langle \mathrm{S}\Psi\lfloor\Psi\mathrm{R}\rangle\end{matrix}\right\}, \end{aligned} \tag{11.15}$$

which is the generalized form of the dimensionless equation (7.14) in Wonacott (1977). The sign of y in this equation is left free when the quadratic equation (11.14) is solved, corresponding to the two possible diffracting positions, but it can be fixed unambiguously by observing that $\angle\psi$ must change sign if R⟩ and X⟩ are interchanged. The sign of y does not have any bearing on whether or not the diffraction condition is satisfied, because the definition of ρ ensures that it is, and (11.14) comprehends only the goniometric conditions. The solution is not always numerically well conditioned even with a double-argument inverse tangent function, since $\eta - y$ and $\epsilon + \rho$ can go to zero simultaneously, so, equivalently, by substitution of $2\cot(\angle\psi/2)/[\cot^2(\angle\psi/2)+1]$ for $\sin\angle\psi$ and $[\cot^2(\angle\psi/2) - 1]/[\cot^2(\angle\psi/2) + 1]$ for $\cos\angle\psi$ we obtain

$$(\rho - \epsilon)\cot^2\frac{\angle\psi}{2} - 2\eta\cot\frac{\angle\psi}{2} + \rho + \epsilon = 0, \tag{11.16}$$

whose solution is

$$\begin{aligned} \angle\psi &= 2\cot^{-1}\left\{\begin{matrix}y + \eta\\ \rho - \epsilon\end{matrix}\right\} \\ &= 2\tan^{-1}\left\{\begin{matrix}\rho - \epsilon\\ y + \eta\end{matrix}\right\} \\ &= 2\tan^{-1}\left\{\begin{matrix}\langle \mathrm{S}\Psi\lfloor\Psi\mathrm{R}\rangle - \langle \mathrm{S}\Psi\lfloor\Psi\mathrm{X}\rangle\\ \langle \mathrm{S}\Psi\rfloor\Psi\mathrm{R}\rangle + \langle \mathrm{S}\Psi\rfloor\Psi\mathrm{X}\rangle\end{matrix}\right\}, \end{aligned} \tag{11.17}$$

where, again, the sign of y is fixed by observing that $\angle\psi$ must change sign if R⟩ and X⟩ are interchanged. This is the only equation in this paper in which the rotationally symmetric operator, $\cdot\lfloor\cdot$, appears in the odd argument of

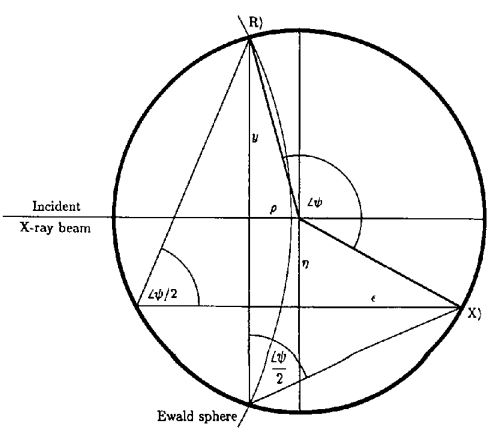

Fig. 8. The half-angle constructions for the Arndt–Wonacott angle. In this diagram the even component is represented horizontally, and the odd component vertically. The radius of the circle is the conventional ξ of the rotation method. The left-hand right-angled triangle represents equation (11.15), the lower right-angled triangle represents equation (11.17). The lightly drawn arc of large radius represents the section of the Ewald sphere intersecting the orbital plane of the reciprocal-lattice vector, X⟩, which comes into the diffracting position at R⟩. This diagram is closely related to Fig. 10, which shows the symmetries more explicitly.

the inverse tangent function and the skew-symmetric operator, $\cdot\lfloor\cdot$, in the even argument. This is not a sign of a mistake, but more an artefact of an implicit rotation through 90° when changing to the cotangent formula: this is seen more clearly if it is noted that $\langle\mathrm{A} = \langle\mathrm{S}\Psi\lfloor\Psi$, $\langle\mathrm{B} = \langle\mathrm{S}\Psi\lfloor\Psi$ and $\bar{\Psi}$ are like mutually perpendicular vectors used as a basis for the calculation; the symmetry of the embedded rotation operators is neither expressed nor relevant. We use (11.15) when $|\eta - y| > |\eta + y|$, and (11.17) otherwise. If $y^2 \leq 0$ then we can set

$$\angle\psi = \angle\tau = \tan^{-1}\begin{Bmatrix}\eta\\ \epsilon\end{Bmatrix} = \tan^{-1}\langle\mathrm{S}\begin{Bmatrix}\Psi\lfloor\Psi\\ \Psi\lfloor\Psi\end{Bmatrix}\mathrm{X}\rangle \quad (11.18)$$

unless $\eta^2 + \epsilon^2 = 0$ when we can set $\angle\psi = 0$. These substitutions, which can be made when the normal form fails, are often computationally very useful, particularly in algorithms for predicting diffraction patterns (Thomas, 1982*a*, chapter 4). Equation (11.18) is related to, but not exactly equivalent to, equation (7.1) of Wonacott (1977).

The geometrical relationships between (11.8), (11.15) and (11.17) are shown in Fig. 8.

12. The dependence of the diffraction angle on variable experimental parameters

The derivatives of the diffraction angle with respect to all of its variable arguments are extremely useful, both during and after collection of diffraction data, since they are required in the equations used to refine estimates of experimental parameters. Derivatives of $\angle\psi$ are evaluated more easily by applying the implicit function theorem to (11.6) than by direct differentiation of explicit forms such as (11.8), (11.15) or (11.17). Using x as a typical parameter, and (11.6) as the implicit function, we can write

$$\frac{\partial\angle\psi}{\partial x} = \frac{-\dfrac{\partial}{\partial x}\left(\dfrac{\langle\mathrm{XX}\rangle}{2} - \langle\mathrm{S}\dot{\Psi}\mathrm{X}\rangle\right)}{\dfrac{\partial}{\partial\angle\psi}\left(\dfrac{\langle\mathrm{XX}\rangle}{2} - \langle\mathrm{S}\dot{\Psi}\mathrm{X}\rangle\right)}. \quad (12.1)$$

The denominator reduces trivially to $-\langle\mathrm{S}\Psi\lfloor\Psi\mathrm{R}\rangle$ by exploiting the differential eigenequation (3.9) of the rotation operator, as indeed in (11.11). The numerator can be recast into a form facilitating the use of the chain rule, so we have

$$\frac{\partial\angle\psi}{\partial x} = \frac{1}{\langle\mathrm{S}\Psi\lfloor\Psi\mathrm{R}\rangle}\left(\langle(\mathrm{X} - \mathrm{S}\dot{\Psi})\frac{\partial\mathrm{X}\rangle}{\partial x} - \langle\mathrm{X}\dot{\Psi}\frac{\partial\mathrm{S}\rangle}{\partial x} - \langle\mathrm{S}\frac{\partial\dot{\Psi}}{\partial x}\mathrm{X}\rangle\right), \quad (12.2)$$

or, more conveniently,

$$\frac{\partial\angle\psi}{\partial x} = \frac{1}{\langle\mathrm{S}\Psi\lfloor\Psi\mathrm{R}\rangle}\left(\langle\mathrm{T}\frac{\partial\mathrm{R}\rangle}{\partial x} - \langle\mathrm{R}\frac{\partial\mathrm{S}\rangle}{\partial x}\right). \quad (12.3)$$

The dependence of the diffraction angle on the scattering vector is important, so substituting $\mathrm{R}\rangle$ for x, we obtain

$$\nabla_{\mathrm{R}\rangle}\angle\psi \equiv \frac{\partial\angle\psi}{\partial\mathrm{R}\rangle} = \frac{\langle\mathrm{T}}{\langle\mathrm{S}\Psi\lfloor\Psi\mathrm{R}\rangle} = \frac{\langle\mathrm{T}}{y}, \quad (12.4)$$

which could be interpreted as the signed Lorentz factor times the radius vector of the Ewald sphere at $\mathrm{R}\rangle$, but is more properly interpreted in terms of the contour surfaces of constant $\angle\psi$ parallel to the surface of the Ewald sphere, which is reflected by $\langle\mathrm{T}$ appearing as a right-acting operator, which behaves like a covector in reciprocal space (Burke, 1985, pp. 18–21; 27–31). Equivalently, uncoupling the rotation through the diffraction angle by using $\mathrm{X}\rangle$, we obtain

$$\nabla_{\mathrm{X}\rangle}\angle\psi \equiv \frac{\partial\angle\psi}{\partial\mathrm{X}\rangle} = \frac{\partial\angle\psi}{\partial\mathrm{R}\rangle}\frac{\partial\mathrm{R}\rangle}{\partial\mathrm{X}\rangle} = \frac{\langle(\mathrm{X} - \mathrm{S}\dot{\Psi})}{\langle\mathrm{S}\Psi\lfloor\Psi\mathrm{R}\rangle} = \frac{\langle\mathrm{T}\dot{\Psi}}{y}, \quad (12.5)$$

which has the same interpretation, but is referred more directly to the crystal. The dependence of the diffraction angle on the incident beam is also important, and is obtained by substitution of $\mathrm{S}\rangle$ for x, giving

$$\nabla_{\mathrm{S}\rangle}\angle\psi \equiv \frac{\partial\angle\psi}{\partial\mathrm{S}\rangle} = \frac{\langle-\mathrm{R}}{\langle\mathrm{S}\Psi\lfloor\Psi\mathrm{R}\rangle} = \frac{\langle\mathrm{R}}{-y}, \quad (12.6)$$

which is minus the signed Lorentz factor times the reciprocal-lattice vector, appearing properly as a covector in reciprocal space with contour surfaces parallel to the diffraction plane at $\mathrm{S}\rangle$. Though the notation is very different, this is the same as the second displayed equation in Thomas (1982*a*), §2.2.2, p. (2.4). The dynamic refinement of variables describing the geometry of the diffraction process during a data-collection run is an iterative procedure, which is most naturally performed using an incremental reconstruction of the conjugate-gradient least-squares algorithm described in §§12–14 of Thomas (1989), presaged by Thomas (1982*a*), §2.3.2 and §§6.5.1–2. When the refinement is done after the completion of the data collection, conventional least-squares optimization procedures are equally appropriate.

The diffraction angle, $\angle\psi$, can be determined much more reliably than the detector position of a spot with currently available area-detector technology, particularly when using the 'diffractometer mode' of data collection (Arndt & Thomas, 1985) and the derivatives quoted above play a dominant role in refinement procedures. The last equation (12.6) can generally be used directly, since $\mathrm{S}\rangle$ is a basic experimental variable, but $\partial\angle\psi/\partial\mathrm{X}\rangle$ (12.5) enters by means of the chain rule of the differential calculus, coupling $\angle\psi$ to the free parameters of the unit-cell matrix, which will usually include explicit orientational terms.

One of the consequences of adopting the tetravariate half-angle notation here would be that the coordinates representing rotations would be homogeneous, and differentials with respect to variations in the direction of axes would be unified with the derivative with respect to the

angle of rotation. This could allow a degree of refinement of axial directions, but such a facility does not appear to be of any utility in area diffractometry.

13. Geometrical interpretations of rotational operators

All of the rotational operators defined in §3 have a natural geometrical interpretation which can be elucidated to some extent by diagrams. However, it is difficult to give concrete representation to the essential conjugacy between left and right forms such as the axis and the sixa. For most purposes, an axis can be represented simply by the line of stasis, drawn as a single straight line. It has no preferred direction, and if the axis is free, no sense of rotation. A signed axis is very similar, but the positive sense of rotation can be denoted by a characteristic symbol such as an arrow wrapped around the line. The conventional metrical representation of an arrow along the line of stasis pointing in the direction in which the rotation appears clockwise would not be acceptable here because it assumes a known chirality of representation.

Although strictly indistinguishable (except by notation) from an axis, a sixa is often most simply represented by a construction based on the orbital planes. Then the law of multiplication of sixa on axis can be demonstrated geometrically by a construction similar to that of covector acting on vector as given, for example, by Burke (1985, pp. 18–21; 27–31). We can start by taking a short segment of the line of stasis and define it to have unit length; this is only of heuristic significance, since no other meaning attaches to the length of the segment. With the sense of positive rotation, this is then a finite geometrical representation of the signed-axis operator. We can then take two orbital planes, one at each end of the axial line segment and including the sense of positive rotation, as a representation of the signed sixa. When a sixa acts on an axis, we can extract a scalar result which is the density of orbital planes perceived by the axial line segment. Thus if the axis and sixa belong to each other the answer is 1 (see Fig. 9*a*), if they belong to exactly antiparallel axes it is -1 (Fig. 9*b*), and all other answers are intermediate (Fig. 9*c*), in conventional notation equal to the cosine of the angle between the axes.

In Cartesian–Euclidean space these simple geometrical constructions suffice. More generally, it is necessary to remember that both axis and sixa comprehend both the line of stasis and the orbital plane, and that the emphasis on one or the other is one of interpretation that we impose for our own convenience; it is not known to the underlying mathematical structure. The act of changing from left-acting to right-acting operators (or *vice versa*) merely swaps the roles of the line of stasis and the orbital plane; thus each of these mutually conjugate operators themselves comprehend both geometrical aspects simultaneously, and can therefore be said to have a self-dual structure.

A more detailed discussion of the differential geometric structure of the rotation operators is beyond the scope of this paper, but the reader will note that it is (*ex hypothesi*) homogeneous and metric-invariant. In other words, the differential structures of, say, E|E or E|E are not materially different from those of E|E or E|E; certainly we no longer worry about why the direction cosines, l, m, n,

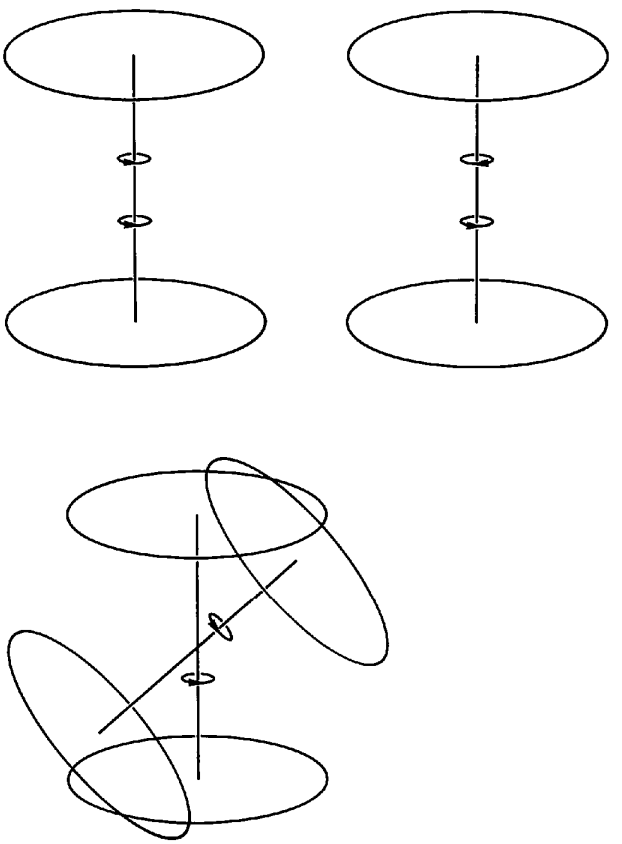

Fig. 9. The action of a sixa on an axis. In many respects these two quantities act upon each other in exactly the same way as do a covector and a vector; however, sixas and axes as defined in this paper comprehend both the covector property and the vector property simultaneously, so a specific geometric assignment can be restrictive. Whilst it is true that for all normal purposes we can choose a Cartesian–Euclidean metric, where the line of stasis is unambiguously normal to any of the orbital planes, it will be noted that under conditions of metric variability (such as those that occur in relativistic transformations, which are essentially equivalent to observing through a distorting imaging system, or a non-linear mapping) the implied right angles will also distort: the abstract operators proposed in this paper survive under these conditions, as does the relationship between the sixa and the axis, whereas the older formalisms based on unit vectors, vector scalar products and perpendicularities fail. These topics are clearly not normally the concern of crystallographers, so it would not be proper to discuss them at greater length here, but the interested reader will find that the beginning of Burke's book of 1985 gives a very clear explanation of the rationale of working in this way. Relativity apart, the techniques of applied differential geometry should not be under-rated, because they have a very powerful effect of exposing the true nature and behaviour of the equations that we use, and very often guide the analyst to simpler and more reliable analytic forms.

appear linearly in the skew-symmetric parts of rotational calculations and quadratically in the symmetric, or about what happens in our computer programs if $l^2 + m^2 + n^2$ accidentally diverges from unity. We can properly regard these as problems of coordinate representation, and not as properties of the underlying rotation.

Concluding remarks

Most calculations can be laborious and difficult if an inappropriate or clumsy representation is chosen for them. I have shown here that an adequate and highly contracted abstract operator notation exists for rotations. This enables the quick and reliable solution of practical problems.

Component representations of the operators are also quoted for substitution into the final answers for numerical computation of the results. In all cases, the most obvious representation in terms of the full angle of rotation is seen to be preferable to the quaternion half-angle representation; the former is simpler and is always numerically well conditioned.

Completely general solutions to three practical calculations have been given: the analytic solution for the three-circle crystal-goniostat is the simplest and fastest known; the calculation of crystal-viewing positions for the kappa-bracket goniostat of the Enraf–Nonius FAST system is new; and the calculation of the Arndt–Wonacott diffraction angle is the only account which is known to be correct in the general case. All of the calculations in this paper have been subjected to extensive experimental verification, being part of the computer program written for the Enraf–Nonius FAST system in Cambridge by the present author. The calculations appropriate for use by area-detector cameras less versatile than the FAST system were also released to the EEC Cooperative Workshop on Position-Sensitive Detector Software held at LURE in Paris in 1986.

I am particularly indebted to Mr J. J. Thomas for drawing my attention to the analysis of rotations in the engineering literature, to Mrs Mary Holmes for her unstinting help in obtaining many of the older references, to Dr P. A. Tucker and especially to Dr R. Diamond for many helpful comments. Most of the computational work leading to this paper was supported by the Medical Research Council of Great Britain as part of the development of the Enraf–Nonius FAST system; the abstract notation was developed during a long illness when I was not in employment, and the manuscript was completed at the European Molecular Biology Laboratory supported by an EMBO long-term fellowship.

APPENDIX

Reductions of the general case

Equation (4.7) is of the form

$$\mathcal{V} = \mathcal{I} + \mathcal{O}\sin\angle e + \mathcal{E}\cos\angle e, \qquad (A1)$$

whose solution, following (4.10) and (4.12), is

$$\angle e = \tan^{-1}\left\{\begin{matrix}\mathcal{O}\\ \mathcal{E}\end{matrix}\right\} \pm \cos^{-1}\left(\frac{\mathcal{V}-\mathcal{I}}{\sqrt{\mathcal{O}^2+\mathcal{E}^2}}\right). \qquad (A2)$$

But we also have the diffraction condition (11.7) in the form of (*A*1), and its solution (11.15) is given in the form

$$\angle e = 2\tan^{-1}\left\{\begin{matrix}\mathcal{O}-\mathcal{W}\\ \mathcal{E}+\mathcal{V}-\mathcal{I}\end{matrix}\right\}, \qquad (A3)$$

where

$$\mathcal{W} = \sqrt{\mathcal{O}^2+\mathcal{E}^2-(\mathcal{V}-\mathcal{I})^2} \qquad (A4)$$

contains the double-valuedness of the solution. It therefore follows that the simpler form of the solution for the Arndt–Wonacott diffraction angle is also available for the solution of the three-circle crystal-goniostat. With this form for the second axis, the general case of the three-circle crystal-goniostat is solved using only three inverse trigonometric functions, one inverse tangent for each axis [*cf.* (4.14), (*A*3) and (4.13) respectively], which is certainly the simplest known, and probably the simplest possible, solution.

These are especially convenient for a well aligned Eulerian cradle, in which $\mathcal{O} = |\Omega X \rfloor X \Phi| = 0$, $\mathcal{E} = |\Omega X \lfloor X \Phi| = 1$ and $\mathcal{I} = |\Omega X | X \Phi| = 0$. For the designed geometry of the kappa-bracket goniostat of the CAD-4 diffractometer, the corresponding values are only slightly less convenient: $\mathcal{O} = |\Omega K \rfloor K \Phi| = 0$, $\mathcal{E} = |\Omega K \lfloor K \Phi| = \sin^2 50°$ and $\mathcal{I} = |\Omega K | K \Phi| = \cos^2 50°$. For very accurate calculations of the positions of real goniostats, which are never perfectly aligned, the equations do not reduce beyond their quoted forms.

The equations discussed in this Appendix are illustrated in Fig. 10.

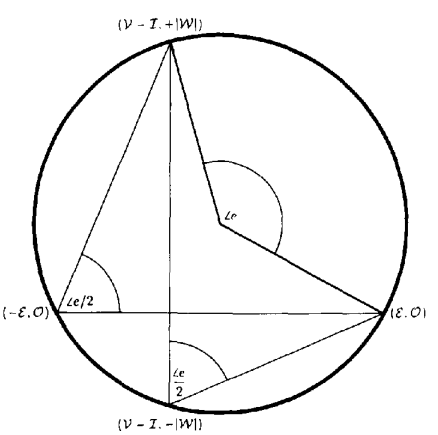

Fig. 10. Full-angle and half-angle forms of the general solution. Like Fig. 8, this diagram has the even components drawn on a horizontal axis, and the odd on a vertical one. The full-angle, $\angle e$, is given by equation (*A*2), the left half-angle, $\angle e/2$, by equation (*A*3), and the lower half-angle, $\frac{\angle e}{2}$, by the corresponding cotangent formula. This diagram is adapted from one suggested by Dr R. Diamond.

References

ARNDT, U.W. & THOMAS, D.J. (1985). Computing aspects of position-sensitive detectors. In *Crystallographic Computing 3: Data Collection, Structure Determination, Proteins, and Databases*, edited by G.M. SHELDRICK, C. KRÜGER & R. GODDARD, pp. 43–51. Oxford: Clarendon Press.

BLÜMLICH, B. & SPIESS, H.W. (1985). Quaternions as a practical tool for the evaluation of composite rotations. *J. Magn. Reson.* **61**, 356–362.

BRAND, L. (1947). Chapter II: Motor algebra, pp. 63–83. See also Chapter X: Quaternions, pp. 403–429. In *Vector and Tensor Analysis*. New York: Wiley.

BRICOGNE, G. (1986). Contribution 9: General parameterization of ψ and flat-film (X,Y) spot coordinates. In *Proceedings of the EEC Cooperative Workshop on Position-Sensitive Detector Software (Phases I & II)* held at LURE, 26 May–7 June 1986, pp. 109–111.

BUERGER, M.J. (1944). The photography of the reciprocal lattice. *Am. Soc. X-ray Electron Diffr.* Monogr. No. 1.

BUERGER, M.J. (1960). Chapter 7: Some geometrical factors affecting intensities. In *Crystal-Structure Analysis*. New York: Wiley.

BURKE, W. L. (1985). *Applied Differential Geometry*. Cambridge Univ. Press.

CLIFFORD, W.K. (1873). Preliminary sketch of biquaternions. *Proc. London Math. Soc.* **4**, 381–395.

DENAVIT, J. (1958). Displacement analysis of mechanisms based on (2×2) matrices of dual numbers. *VDI Ber. (Ver. Dtsch. Ing.)*, **29**, 81–88.

DIAMOND, R. (1988). A note on the rotational superposition problem. *Acta Cryst.* A**44**, 211–216.

DIAMOND, R. (1990). On the factorisation of rotations with examples in diffractometry. *Proc. R. Soc. London Ser. A*, **428**, 451–472.

Дментберг, Ф. М. (1948). **Общий метод исследования конечных перемещений пространственных механизмов и некоторые случаи пассивных связей**. [A general method for the investigation of finite displacements of spatial mechanisms and certain cases of passive constraints.] **Труды Семинара по теории машин и механизмов** [*Workshop on theory of machines and mechanisms*], **Акад. наук СССР**, 5, 5–39.

DIMITRIĆ, R. & GOLDSMITH, B. (1989). Sir William Rowan Hamilton. *The Mathematical Intelligencer*, **11**, 29–30.

DIRAC, P.A.M. (1958). *The Principles of Quantum Mechanics*, 4th ed., §§5–6, pp. 14–22. Oxford Univ. Press.

EULER, L. (1758). Du mouvement de rotation des corps solides autour d'un axe variable. *Mém. Acad. Sci. Berlin*, **14** (1765), 154–193. = *Opera omnia*, ser. 2 (*Opera mechanica*, edited by CHARLES BLANC), **8**, 200–235. Zurich: Orell Füssli (1964).

EULER, L. (1765). Chapter XI: De motu libero corporum rigidorum ternis axibus principalibus paribus praeditorum et a nullis viribus sollicitatorum—Theorema 9, §690, 277–278. In *Theoria motus corporum solidorum seu rigidorum—Statica*. = *Opera omnia*, ser. 2, **4**, 4–6. Berne (1950).

EULER, L. (1775*a*). Formulæ generales pro translatione quacunque corporum rigidorum. *Nov. Comm. Acad. Sci. Petrop.* **20** (1776), 189–207; *Summarium ibidem*: 26–28. = *Opera omnia*, ser. 2, **9**, 84–98. Basle (1968).

EULER, L. (1775*b*). Nova methodus motum corporum rigidorum determinandi. *Nov. Comm. Acad. Sci. Petrop.* **20** (1776), 208–238; *Summarium ibidem*: 29–33. = *Opera omnia*, ser. 2, **9**, 99–125. Basle (1968).

GAUSS, C.F. (1819). Mutationen des Raumes. *Werke*, **8**, 357–362. Published in 1900.

GOLDSTEIN, H. (1950). §4-4, The Eulerian angles, pp. 107–109, §4-5, The Cayley–Klein parameters, pp. 109–118. In *Classical Mechanics*, 1st ed. Reading, MA: Addison-Wesley.

GOLDSTEIN, H. (1980). §4-4, The Euler angles, pp. 143–148, §4-5, The Cayley–Klein parameters and related quantities, pp. 148–158. In *Classical Mechanics*, 2nd ed. Reading, MA: Addison-Wesley.

GRAY, J.J. (1980). Olinde Rodrigue's paper of 1840 on transformation groups. In *Archive for History of Exact Sciences*, Vol. 21, pp. 375–385. Berlin: Springer-Verlag.

HAMILTON, W.R. (1843*a*). Quaternions [manuscript]. In *The Mathematical Papers of Sir William Rowan Hamilton*, Vol. III, edited by H. HALBERSTAM & R.E. INGRAM, pp. 103–105. Cambridge Univ. Press (1967).

HAMILTON, W.R. (1843*b*). Letter to Graves on quaternions; or on a new system of imaginaries in algebra. *Philos. Mag.* **25** (1844), 489–495. In *The Mathematical Papers of Sir William Rowan Hamilton*, Vol. III, edited by H. HALBERSTAM & R.E. INGRAM, pp. 106–110. Cambridge Univ. Press (1967).

HAMILTON, W.R. (1844). On a new species of imaginary quantities connected with the theory of quaternions. *Proc. R. Irish Acad.* **2**, 424–434. In *The Mathematical Papers of Sir William Rowan Hamilton*, Vol. III, edited by H. HALBERSTAM & R.E. INGRAM, pp. 111–116. Cambridge Univ. Press (1967).

HAMILTON, W. R. (1853). On the geometrical interpretation of some results obtained by calculations with biquaternions. *Proc. R. Irish Acad.* **5**, 388–390. In *The Mathematical Papers of Sir William Rowan Hamilton*, Vol. III, edited by H. HALBERSTAM & R. E. INGRAM, pp. 424–425. Cambridge Univ. Press (1967).

HESTENES, D. (1986). A unified language for mathematics and physics. In *Clifford Algebras and Their Applications in Mathematical Physics*, edited by J.S.R. CHISHOLM & A.K. COMMON, pp. 1–23. Dordrecht: Reidel.

HESTENES, M.R. & STEIFEL, E. (1952). Methods of conjugate gradients for solving linear systems. *J. Res. Natl Bur. Stand.* **49**, 409–436.

KLEIN, F. (1884*a*). *Vorlesungen über das Ikosaeder. . .* (Leipzig). = *Lectures on the Icosahedron and the Solution of Equations of the Fifth Degree*, 2nd ed. (in English translation), Chapter 1, §1, p. 5. London: Kegan Paul, Trench, Trübner (1913).

KLEIN, F. (1884*b*). *Vorlesungen über das Ikosaeder. . .* (Leipzig). = *Lectures on the Icosahedron and the Solution of Equations of the Fifth Degree*, 2nd ed. (in English translation), Chapter 2, §§1–3, pp. 31–39. London: Kegan Paul, Trench, Trübner (1913).

LIPSON, H. (1972). *International Tables for X-ray Crystallography*, Vol. II, p. 266, third equation (18). Birmingham: Kynoch Press. (Present distributor Kluwer Academic Publishers, Dordrecht.)

MESSERSCHMIDT, A. (1986). New parameterisation as applied to the FAST detector. In *Proceedings of the EEC Cooperative Workshop on Position-Sensitive Detector Software (Phase III)* held at LURE, 12–19 November 1986, pp. 63–64.

MILCH, J.R. & MINOR, T.C. (1974). The indexing of single-crystal X-ray rotation photographs. *J. Appl. Cryst.* 7, 502–505.

MISNER, C.W., THORNE, K.S. & WHEELER, J.A. (1973). Chapter 41: Spinors, pp. 1135–1165. In *Gravitation*. San Francisco: W.H. Freeman.

NEWTON, I., (1669). *De Analysi per æquationes numero terminorum infinitas*. Original in the Library of the Royal Society of London. Reproduced with English translation in *The Mathematical Papers of Isaac Newton*, Vol. II, pp. 206–247, edited by D.T. WHITESIDE. Cambridge Univ. Press.

POOT, S. (1972). Goniometric apparatus for an X-ray diffractometer. United States Patent 3,636,347.

RAPHSON, J. (1690). *Analysis Æquationum UNIVERSALIS*, SEU *Ad ÆQUATIONES ALGEBRAICAS Resolvendas METHODUS Generalis, et Expedita, Ex nova Infinitarum serierum Doctrina, DEDUCTA* AC *DEMONSTRATA*. Original in the British Library, London.

RODRIGUES, O. (1840). Des lois géométriques qui régissent les déplacements d'un système solide dans l'espace, et de la variation des coordonnées provenant de ces déplacements considérés indépendamment des causes qui peuvent les produire. *J. Math. (i.e. Journal de Liouville, 1 série)*, **5**, 380–440.

TAIT, P.G. (1890). *An Elementary Treatise on Quaternions*, 3rd ed. Cambridge Univ. Press.

THOMAS, D.J. (1982*a*). Fast Diffractometry. PhD thesis. Cambridge University, England.

THOMAS, D.J. (1982*b*). High-speed single-crystal television diffractometer (software). *Nucl. Instrum. Methods*, **201**, 27–30.

THOMAS, D.J. (1985). Computing for the Enraf–Nonius FAST system. In *Crystallographic Computing* 3: *Data Collection, Structure Determination, Proteins, and Databases*, edited by G.M. SHELDRICK, C. KRÜGER & R. GODDARD, pp. 52–60. Oxford: Clarendon Press.
THOMAS, D. J. (1989). Calibrating an area-detector diffractometer. Imaging geometry. *Proc. R. Soc. London Ser. A*, **425**, 129–167.
THOMAS, D.J. (1990*a*). Calibrating an area-detector diffractometer. Integral response. *Proc. R. Soc. London Ser. A*, **428**, 181–214.
THOMAS, D.J. (1990*b*). Modern equations of diffractometry. Diffraction geometry. In preparation.
WONACOTT, A.J. (1977). Geometry of the rotation method. In *The Rotation Method in Crystallography*, edited by U. W. ARNDT & A. J. WONACOTT, pp. 75–103. Amsterdam: North-Holland.
YANG, A.T. (1969). Displacement analysis of spatial five-link mechanisms using (3×3) matrices with dual number elements. *Trans. ASME*, **91(B)** (*J. Eng. Ind.*), 152–157.
YANG, A.T. & FREUDENSTEIN, F. (1964). Application of dual-number quaternion algebra to the analysis of spatial mechanisms. *Trans. ASME*, **86(E)** (*J. Appl. Mech.*), 300–308.

Acta Cryst. (1990). A**46**, 343-351

Determination of Electrostatic Potentials in Crystalline Compounds. The Application to Boric Acid

BY PETER SOMMER-LARSEN,* ANDERS KADZIOLA AND MICHAEL GAJHEDE

Department of Physical Chemistry, The HC Ørsted Institute, University of Copenhagen, DK-2100 Copenhagen, Denmark

(*Received* 28 *June* 1989; *accepted* 15 *November* 1989)

Abstract

A formalism for deriving electrostatic potentials in crystals is presented, with emphasis on the choice of origin and the determination of the mean inner potential. Conditions for applying the conventional origin chosen for isolated molecules are specified. The formalism is applied to orthoboric acid, and maps of the electrostatic potentials are presented. Extinction appears to be a severe problem in mapping electrostatic potentials, and its effects are investigated with a multipole expansion of the electron density. The effects of thermal motion are seen to be small at points far from the atomic core regions.

Introduction

It has been shown that electrostatic potentials in crystals can be derived from X-ray diffraction data (Stewart, 1979). This paper will present our application of this formalism. Even though electrostatic potentials are of major importance in the investigation of chemical dynamics, only a few groups work, or have worked, with the mapping of potentials from diffraction data (Moss & Coppens, 1980; Moss & Feil, 1981; Feil & Moss, 1983; Stewart, 1982; Swaminathan, Craven & McMullan, 1985). Bertaut (1952, 1977) has worked with the mapping of potentials in ionic crystals.

The most frequently applied method for determining electrostatic potentials from crystallographic data (*e.g.* Swaminathan, Craven & McMullan, 1985) is based on a multipole expansion of the electron density. So far, this method has been used to derive the potential of a single molecule from the multipole functions and the expansion coefficients.

In this paper we concentrate on the potential inside a crystal. The first section discusses the distinction between the electrostatic potential in a crystal, calculated either by a Fourier sum in reciprocal space or by a superposition in direct space of the potentials from the units which build up the crystal. The charge density of such a unit - the building block for the crystal - could be the charge density inside a single unit cell or it could be the charge density from the atoms or molecules in the unit cell.

The Fourier coefficient of the potential for the reciprocal-lattice vector of length zero is of special importance when discussing the two different ways of expressing the potential as this coefficient is the average value of the potential inside the crystal. It is known as the mean inner potential. Changing this Fourier coefficient corresponds to changing the origin for the potential inside the crystal. So in the first section we pay special attention to the question of how to determine the origin of the potential and how to calculate the mean inner potential. An important part of this section is found in Appendix *A*.

In the second chapter we discuss some of the potential maps and the chemical information which can be derived from X-ray diffraction data. Both maps of the potential in a crystal and the potential of a single molecule and their relations are discussed.

The actual calculations deal only with the potential in a crystal. We use the algorithm of Stewart (1982)

* Present address: Department of General Chemistry, Royal Danish School of Pharmacy, Universitetsparken 2, DK-2100 Copenhagen, Denmark.

0108-7673/90/050343-09$03.00